

Contents lists available at ScienceDirect

Journal of Energy Chemistry

http://www.journals.elsevier.com/

journal homepage: www.elsevier.com/locate/jechem

Review

Research progress on silicon/carbon composite anode materials for lithium-ion battery

Xiaohui Shen^b, Zhanyuan Tian^{a,b,*}, Ruijuan Fan^b, Le Shao^b, Dapeng Zhang^b, Guolin Cao^b, Liang Kou^b, Yangzhi Bai^b

ARTICLE INFO

Article history: Received 7 June 2017 Revised 7 December 2017 Accepted 19 December 2017 Available online 22 December 2017

Keywords: Lithium-ion batteries Anodes Silicon/carbon composite

ABSTRACT

Silicon (Si) has been considered as one of the most promising anode material for the next generation lithium-ion batteries (LIBs) with high energy densities, due to its high theoretical capacity, abundant availability and environmental friendliness. However, silicon materials with low intrinsic electric and ionic conductivity suffer from huge volume variation during lithiation/delithiation processes leading to the pulverization of Si and subsequently resulting in severe capacity fading of the electrodes. Coupling of Si with carbon (C) realizes a favorable combination of the two materials properties, such as high lithiation capacity of Si and excellent mechanical and conductive properties of C, making silicon/carbon composite (Si/C) ideal candidates for LIBs anodes. In this review, recent progresses of Si/C materials utilized in LIBs are summarized in terms of structural design principles, material synthesis methods, morphological characteristics and electrochemical performances by highlighting the material structures. The mechanisms behind the performance enhancement are also discussed. Moreover, other factors that affect the performance of Si/C anodes, such as prelithiation, electrolyte additives, and binders, are also discussed. We aim to present a full scope of the Si/C-based anodes, and help understand and design future structures of Si/C anodes in LIBs.

© 2018 Science Press and Dalian Institute of Chemical Physics, Chinese Academy of Sciences. Published by Elsevier B.V. and Science Press, All rights reserved.



Xiao Hui Shen is a researcher of New Energy Technology Department, Shaanxi Coal and Chemical Technology Institute Co., Ltd. She achieved her Master of Engineering degree from Tianjin University in 2013. Her research interest is the silicon-based composites as negative electrode for high energy lithium ion batteries.



Zhan Yuan Tian is a researcher of New Energy Technology Department, Shaanxi Coal and Chemical Technology Institute Co., Ltd. And he is currently studying for a Ph.D. degree from Xi'an Jiaotong University. He received his Master of Engineering degree from Zhejiang University in 2010. His research interests focus on the negative and positive materials and the rational design for lithium ion batteries.



Rui Juan Fan is a researcher of New Energy Technology Department, Shaanxi Coal and Chemical Technology Institute Co., Ltd. She achieved MS degree from Central South University in 2013. Her research interests focus on lithium ion batteries, especially the silicon-based composites as negative electrode for high energy.

E-mail address: tianzy@sxccti.com (Z. Tian).

^a Center of Nanomaterials for Renewable Energy, State Key Laboratory of Electrical Insulation and Power Equipment, School of Electrical Engineering, Xi'an Jiaotong University, Xi'an 710049, Shaanxi, China

^b Shaanxi Coal and Chemical Technology Institute Co., Ltd., Xi'an 710070, Shaanxi, China

Corresponding author.



Le Shao is a researcher of New Energy Technology Department, Shaanxi Coal and Chemical Technology Institute Co., Ltd. He received his Ph.D. degree from Shanghai Institute of Ceramics, Chinese Academy of Sciences in 2013. He works on the design and manufacturing for lithium ion batteries.



Da Peng Zhang is a researcher of New Energy Technology Department, Shaanxi Coal and Chemical Technology Institute Co., Ltd. He achieved his Ph.D. degree from Tianjin University in 2014. His research interest is the silicon and silicon compounds as anode materials for high energy lithium ion batteries.



Guo Lin Cao is a researcher of New Energy Technology Department, Shaanxi Coal and Chemical Technology Institute Co., Ltd. He achieved MS degree from Beijing Institute of Technology in 2015. His research interests focus on lithium ion batteries, nano energy materials and photoelectrochemical water splitting.



Liang Kou received his Ph.D. degree in 2014 from Polymer Chemistry and Physics at Zhejiang University under the direction of Prof. Chao Gao. Now he is a research scientist in Shaanxi Coal and Chemical Technology Institute Co., Ltd. His research interests focus on the synthesis and mass production of cathode, anode materials for lithium battery.



Yangzhi Bai is a researcher of New Energy Technology Department, Shaanxi Coal and Chemical Technology Institute Co., Ltd. She achieved MS degree from Dalian Institute of Chemical Physics, Chinese Academy of Sciences in 2016. Her research interest is the silicon and silicon compounds as anode materials for high energy lithium ion batteries.

1. Introduction

In the last two decades, the lithium-ion batteries (LIBs) have successfully dominated the portable electronic market and exhibit great promise for vehicle electrification [1]. The techniques have developed rapidly and the energy density is enhanced at a rate of $7\%\sim10\%$ per annum. However, it is still far below the specific energy requirement for electric vehicles (EVs). Graphite, as the anode material in commercial LIBs, has almost reached its theoretical specific capacity of 372 mAh/g and can only offer a specific energy of $\sim150\,\mathrm{Wh/kg}$, which is insufficient to match the specific energy requirement for EVs in order to match the performance of internal combustion vehicles [2]. In addition, currently, our country's "energy saving and new energy vehicle technology roadmap" promulgates that the goal of specific energy for EVs must be up to 350 Wh/kg in 2020. Therefore, novel anode materials are urgent to

be researched and exploited for the application of next-generation LIBs.

Silicon has attracted a great deal of attentions as one of the most promising anode candidates to replace commercial used graphite because of its obvious advantages, such as a theoretical capacity of 3590 mAh/g based on fully alloyed form of Li₁₅Si₄, an attractive working potential (~0.4 V versus Li/Li+) associated with slightly higher than that of graphite (~0.05 V versus Li/Li+) as well as better environmental friendliness and abundance [3,4]. Unfortunately, practical application of Si anodes is currently hampered by multiple challenges. The primary is its huge volume change (~300%) upon full lithiation and the resultant expansion/shrinkage stress during lithiation/delithiation, which induces severe cracking of Si. That results in the formation of an unstable solid electrolyte interphase (SEI) on the Si surface, and causes lithium trapping in active Si material, consequently leading to irreversible fast capacity loss and low initial coulombic efficiency (CE). Moreover, the slow lithium diffusion kinetics in Si (diffusion coefficient between 10^{-14} and 10^{-13} cm²/s) and low intrinsic electric conductivity of Si $(10^{-5}-10^{-3} \text{ S/cm})$ also significantly affect the rate capability and full capacity utilization of Si electrodes [5-8]. These issues have to be addressed before the practical application of Si

Significant efforts have been undertaken to tackle these issues mentioned above. For example, moving from bulk to nanoscale morphologies have the potential to solve the expansion/shrinkage stress of Si during lithiation/delithiation in some degree. Such nanoscale dimensions allow quick relaxation of stress, making nano-sized Si more resistant to fracture than bulk particles. A strong particle-size-dependent fracture behavior of Si particles during the first lithiation is discovered; that is, there exist a critical particle diameter of about 150 nm, below which the particles neither crack nor fracture, and above which the particles initially form surface cracks upon lithiation and then fracture due to lithiation-induced swelling [9]. Besides, nanostructured Si materials also possess other benefits, including short lithium diffusion distances within the electrode, enhanced mass transport along surfaces and grain boundaries, and high rate capability due to the large surface area. However, nanostructured Si materials also face some formidable challenges accompanied by its high surface area and surface-to-volume ratios, including limiting irreversible capacity and low coulombic efficiency, which are caused by the formation of a passivation layer or solid electrolyte interface (SEI) layer on the electrode surface [10]. Another most successful strategy among them is to incorporate other components, especially carbon mediums, which act as stress buffering matrices into Si to accommodate the strain. Carbonaceous materials possess superior mechanical property and high electron and ion transport rate. And there are chemical similarities with Si, leading to a compact contact upon combination of silicon with carbon matrix. In this composite system, silicon materials act as active components contributing to high lithium storage capacity while carbon matrix can significantly buffer volume expansion of Si and improve electronic conductivity and stabilize the SEI layers of the Sibased anodes [11-13]. Hence, coupling of nano-sized Si with carbon proves to be an effective method of improving capacity, cycling stability and initial CE of the electrodes by alleviating the volume change of Si and minimizing the fracture and re-formation of SEI

In order to further enhance the performance of Si anodes, electrolyte additives, binders and prelithiation treatment should also be considered. The introduction of appropriate additives is beneficial to the formation of thin and stable SEI layers, so as to reduce the consumption of extra electrolyte during cycling and lead to better cycling stability. Polymer binders are components used in preparing electrodes, which are usually mixed with active materi-

als and conductive additives to form slurries in order to form relatively homogeneous and stable coatings on current collectors. The selection of suitable polymer binders can enhance the integrity of Si electrodes. In addition, the prelithiation treatment compensates for lithium consumption during the SEI formation process, hence resulting in remarkably increased reversible capacity and coulombic efficiency, particularly in the first cycle [4,13].

In this review, we summarize the up-to-date advances in Si/C anode materials. Special focuses are given to structure designs, synthetic routes and electrochemical performances of these Si/C composites. The innovative electrode structures including coreshell structure, yolk–shell structure, porous structure, and embedding structure, etc., are focused here, while carbonaceous matrixes (amorphous carbon, graphite, carbon nanowire/nanotube, graphene, etc.) composited with Si to improve the electrochemical performance are also discussed. Other factors that affect the performance of Si/C anodes, such as electrolyte additives, binders, and prelithiation treatment, are also presented. In a word, we hope that our review will be able to stimulate further discussions and ideas on the rational design of durable and high performance Si/C anodes for the next generation Li-ion batteries in future.

2. Designed structures

Si/C composites are generally prepared based on silicon sources and various carbon raw materials by shaping and sintering. The Si–C coupling can realize a favorable combination of high specific capacity of Si and alleviate the large volume change of Si upon cycling for structural integrity of the electrode. Si/C composites-based structures are generally classified into four categories, including core–shell structure, yolk–shell structure, porous structure and embedding structure. Among them, a portion of well-designed Si anodes, such as carbon coating (core–shell structure), pomegranate-inspired Si design (yolk–shell structure), micro-sized porous Si (porous structure) and graphene-supported (embedding structure), have demonstrated the possibility of achieving high specific capacities with long life as well as high areal capacities (>3.0 mAh/cm²) with high Si mass loading, which is essential for practical application of LIBs [4].

2.1. Core-shell structure

Core-shell Si/C composites are synthesized by entirely covering/encapsulating a solid Si core with a conductive carbon shell. The carbon shell offers some advantages: (1) enhances electronic conductivity: (2) provides mechanical support to accommodate the volume expansion of Si during lithium insertion/extraction; (3) isolates Si core from electrolyte and in turn decreases the occurrence of side reactions with the electrolyte so as to stabilize the SEI layers and improve the initial CE. Zhang et al. [14] prepared Si/C composite with core-shell structure (Si@C) through emulsion polymerization of acrylonitrile in the presence of Si nanoparticles (Si NPs), followed by pyrolysis process. The presence of amorphous carbon shell prevented the agglomeration of tiny Si NPs during charge/discharge cycles, thus improved the cycling performance of the electrode. Compared with bare Si, the capacity of which faded quickly after 20 cycles, the Si@C composite retained half of its initial capacity. Similarly, Hwa et al. [15] fabricated Si@C core-shell composite with a carbon shell thickness of 5-10 nm by pyrolyzing polyvinyl alcohol (PVA). The Si@C composite maintained a capacity of 1800 mAh/g after 50 cycles at 100 mA/g, whereas the capacity of pure Si particles faded less than 200 mAh/g after the same number of cycles. Wang et al. [10] have compared the performance of nano-sized Si (\sim 0.15 μm) with those of micro-sized Si particles (1-2μm) with and without carbon coating. Their study clearly indicated that the nano-sized Si had a higher specific capacity and

better capacity retention than those of the micro-sized Si, while the carbon-coated, nano-sized Si possessed the best performance. Specifically, the micro-sized Si exhibited a specific capacity of 650 mAh/g after 100 cycles at 100 mA/g and its capacity retention was only 20% when compared with the first charge capacity. In contrast, the nano-sized Si displayed a capacity of 1060 mAh/g after 100 cycles with its capacity retention of 38%. Here, such set of data unambiguously revealed that capacity retention of Si could be improved by reducing its particle size, which was mainly attributed to the reduced tendency for particle cracking and smaller volume change of Si particle during cycles. Moreover, the carbon coating could further improve the capacity retention because of the buffering effect of the coating.

It is noticeable that such core-shell structure mentioned above can enhance the cycling behavior of Si based anode. In addition, the species source and shell structure of carbon play an important role in determining the properties of Si@C core-shell composite system. Liu et al. [16] synthesized various Si/C composites with core-shell structures through pyrolysis of different carbon source including sucrose, resin, polyoxyethylene (PEO), polyvinyl chloride (PVC), polyethylene (PE), chlorinated polyethylene (CPE), pitch and polyvinylidene fluoride (PVDF). It was found that the Si-pyrolyzed PVDF composite displayed the optimal morphological stability. The authors attributed such advantage to the strong etching of fluorine to silicon during pyrolysis process, which inserted part of fluorine into Si-Si bond and thus strengthened the interface compatibility between carbon shell and silicon core. It was concluded that the carbon shell doped with elements was a benefit for constructing a more compact and stable interface between carbon and silicon, thus a better electrochemical performance was obtained. Recently, another study on the Si/ graphite@N-doped carbon core-shell composite was executed by Zhou et al. [17]. The silicon/graphite particles were obtained through liquid mixing and spray-drying process. In the next step, the spherical silicon/graphite particles were coated during oxidative self-polymerization of dopamine. And the Si/graphite@N-doped carbon composite was formed finally through subsequent pyrolysis. The N-doped carbon layer can not only prevent the direct contact between Si and electrolyte, but also serve as buffer for the volume expansion of Si/graphite core during lithiation/delithiation process. Moreover, N-doped carbon could both improve electronic conductivity of Si material and accelerate the transportation of Li⁺. The composite exhibited an initial reversible capacity of 741.2 mAh/g at 300 mA/g while a high reversible capacity of 611.3 mAh/g was delivered after 100 cycles.

Porous carbon layer has also been introduced as conductive matrix to composite with Si core in order to acquire improved capacity and stability. The unique porous structure of carbon layer offers space for the volume expansion of Si core during charge/discharge process. Besides, it can also facilitate the Li⁺ and electrons transport, thus decrease the charge transfer resistance. Shao et al. [18] prepared nanostructured silicon/porous carbon spherical composite (N-SPC) by hydrothermal process and soft template method, using glucose as carbon source and pluronic F127 as pore forming agent in the presence of Si NPs, as summarized in Fig. 1(a). The N-SPC composite displayed favorable electrochemical kinetics owing to the nano-sized porous carbon shell. Such porous structure facilitated the formation of a solid electrolyte interface film and the transportation of electrons and Li ions. Consequently, the composite exhibited excellent cycling stability and rate capability, delivering a stable capacity of 1607 mAh/g at 0.4 A/g after 100 cycles with a capacity retention of 85.0% (Fig. 1b), and a reversible capacity of 1050 mAh/g even at a high current density of 10 A/g (Fig. 1c). Similarly, silicon@porous nitrogen-doped carbon spheres anodes using melanin-formaldehyde resin as carbon source also exhibited outstanding reversible capacity of 1579 mAh/g at C/10 and 94% capacity retention after 300 cycles [19].

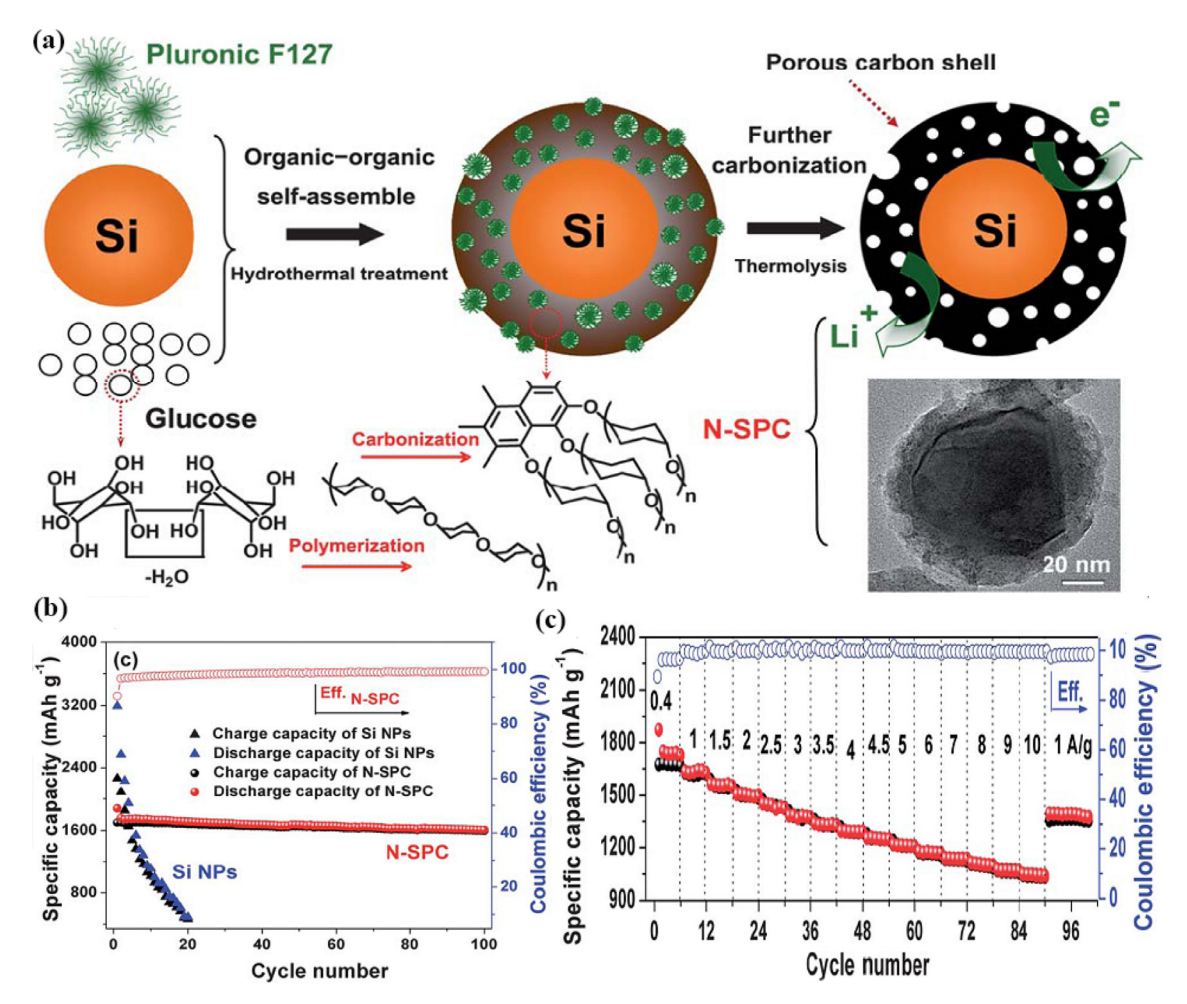


Fig. 1. (a) Schematic illustration of the synthesis of monodisperse nanostructured silicon/porous carbon spheres; (b) Cycling performance of N-SPC at a constant current density of 0.4 A/g; (c) The rate performance of N-SPC measured at various current densities from 0.4 to 10 A/g. Reprinted with permission from Ref. [18]. Copyright (2013) Royal Society of Chemistry.

Accordingly, it is found that such core-shell structure by conductive carbon shell on the surface of Si particles can improve the cycle stability. Nevertheless, the advantages are limited in some situations since a tremendous volume change of Si core during lithiation still leads to inevitable volume expansion of the entire core-shell composites. The induced fracture of carbon shell will expose Si core to the electrolyte, thus giving rise to the formation of SEI layer and finally collapsing the electrode structure. It is noticeable that excellent mechanical properties of conductive carbon shell is essential to suppress the volume expansion of Si core, in order to form more stable interface between particles and minimize fracture of SEI layer. To solve this issue, a double-walled core-shell structure has been designed and fabricated by Tao et al. [20]. In this case, Si NPs were coated with double shells, silicon dioxide (SiO₂) and pyrolytic carbon, and the obtained material was denoted as Si@SiO2@C. Compared to single core-shell structure (Si@C), the Si@SiO2@C composite displayed more stable cycling behavior between 0.01 V and 5.0 V, yielding a reversible capacity of 785 mAh/g after 100 cycles at 100 mA/g with a loss of 0.13% per cycle. It was corroborated that the thin SiO₂ interlayer enhanced the adhesion of carbon shell to the Si core and alleviated stresses of Si during cycling. In addition, SiO₂ shell could react with Li⁺ irreversibly to form Li₄SiO₄ alloy and Si. The generated Si was beneficial for reversible capacity of the composite while Li₄SiO₄ alloy could further provide mechanical support to inhibit volume expansion of Si core.

Taking all of the aforementioned results together, it can be concluded that Si/C-based composites with desired properties of stable cycling stability and high coulombic efficiency can realize as long as the following conditions are taken into account: (i) the size of Si core with nano-structured, (ii) the conductive and electrochemically carbon shell, and (iii) appropriate synthesis factors to achieve a uniform and mechanically strong shell.

2.2. Yolk-shell structure

Based on the solid Si@C core-shell structure, a new class of Si/C multiphase nano-composites with yolk-shell structure is exploited via introduction of additional internal void spaces between silicon core and carbon shell. The yolk-shell structure consists of Si particles completely protected by a thin layer of carbon which facilitate the Li ion and electron transfer and offer a stable interface for good contact between particles. The voids inside the yolk-shell structures provide an effective way to buffer the volume expansion and allow the Si core to freely expand and shrink without pulverization. This smart design will be more beneficial to the formation of stable SEI layer and maintain the integrity of the electrode.

The Si/C composites with yolk–shell structures are usually prepared by template-based approaches which consist of three steps: (1) synthesis of templates; (2) deposition of carbon on the templates; and (3) removal of the templates by etching or calcination. Therein, SiO_2 is the most common template. Zhou et al.

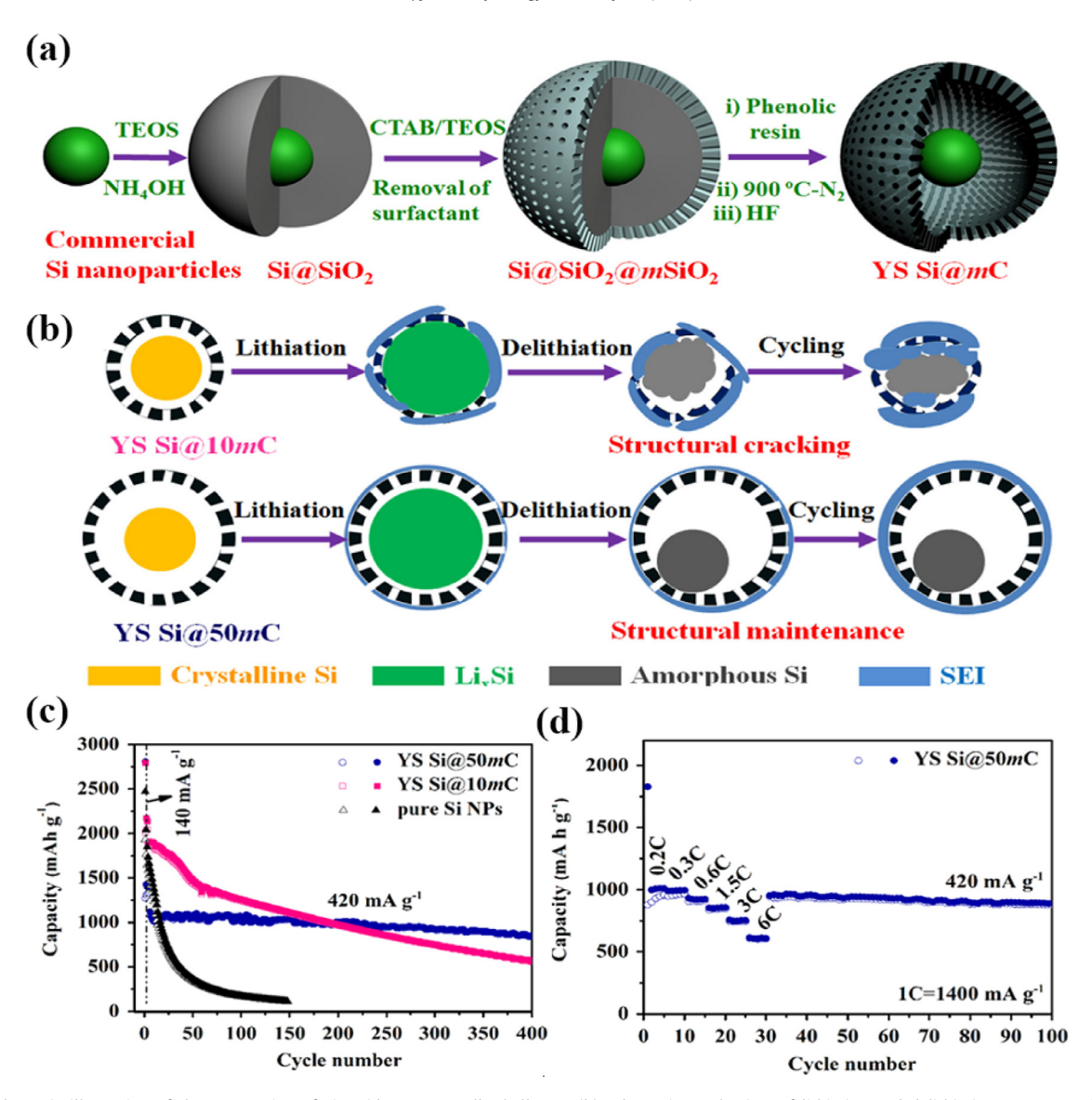


Fig. 2. (a) Schematic illustration of the preparation of Si@void@meso-C yolk-shell NPs; (b) Schematic mechanism of lithiation and delithiation processes of YS Si@10mC and YS Si@50mC electrodes; (c) Cycling performance of YS Si@50mC, YS Si@10mC, and commercial SiNPs electrode; (d) Rate performance of YS Si@50mC. Reprinted with permission from Ref. [23]. Copyright (2015) Published by Elsevier Ltd.

[21] synthesized Si@void@C yolk-shell structure through coating Si NPs with a SiO₂ sacrificial layer via hydrolysis of tetraethoxysilane (TEOS), followed by deposition of pyrolytic carbon. Hydrofluoric acid (HF) was used to leaching out the SiO₂ components, leading to formation of Si@void@C yolk-shell structure. The yolk-shell electrode possessed higher cycle stability than Si NPs and hollow carbon, which delivered 813.9 mAh/g in the first cycle and retained about 500 mAh/g after 40 cycles. Using similar method, Tao et al. [22] also synthesized the Si@void@C yolk-shell structure, and acquired an exceedingly stable Si/C nanocomposite with capacity decay as small as 0.02% per cycle.

Yang et al. [23] devised unique yolk–shell silicon-mesoporous carbon structures via a template-based method and a nanocasting strategy, the schematic illustration of the fabrication process was displayed in Fig. 2(a). An SiO₂ layer was coated on the surface of Si NPs, followed by uniform coating of mesoporous SiO₂ shells with the assistance of hexadecyltrimethylammonium bromide (CTAB) as a porogenic agent. Then phenolic resin precursor was impregnated into the mesopore channels via a capillary force. After carbonization and selective removing silica by HF etching,

Si@void@meso-C structures were obtained. In this structure, the individual Si NPs were encapsulated by open and accessible mesoporous carbon layers instead of solid carbon layers. Apart from the void space offering enough room for accommodating volume expansion, the porosity of carbon shell enabled fast transport of Li⁺ between electrolyte and silicon yolk. Further, they have examined the effect of void space in such yolk-shell structure, and found that the composite with ~10 nm void space (YS Si@10mC) displayed structural degradation after 100 cycles, whereas the composite with ~50 nm void space (YS Si@50mC) retained its original structure well (Fig. 2b). It was suggested that sufficient void space was needed to tolerate the volume change of internal Si yolk without causing the carbon shell fracture. Thus, the capacity retention of YS Si@10mC only remained at 27.7% over 400 cycles, whereas YS Si@50mC was capable of delivering a constant capacity (~1000 mAh/g), in which the capacity retention was as high as 78.6% after 400 cycles (Fig. 2c). Apart from predominant cycling stability, YS Si@50mC also possessed superior rate capability of 62.3% capacity retention even at a current density of 8.4 A/g (Fig. 2d).

Recently, a novel kind of yolk-shell Si@C@void@C nanocomposites were proposed and studied by Xie et al. who fabricated this nanostructure from commercial nano-Si particles [24]. A uniform carbon layer was coated on the surface of Si NPs by carbonization of polydopamine. Subsequently, the addition of TEOS resulted in the formation of core-double-shell Si@C@SiO2 nanostructure via sol-gel process. The Si@C@SiO2 template was then re-coated with a polydopamine, and a following pyrolysis and HF etching process led to the generation of final Si@C@void@C structure (Fig. 3a). Compared with Si@void@C materials, the resultant Si@C@void@C structure introduced Si@C particles severing as yolks instead (Fig. 3b-g). Such additional internal carbon shell could provide better electronic transport between Si cores and external carbon shells, leading to much smaller charge-transfer impedance than Si@void@C. Meanwhile, the internal and external carbon shells worked together to entirely cover Si cores effectively, so as to prevent the electrolyte from reaching the surface of Si NPs and thus prohibited electrode from subsequent irreversible reaction with electrolyte. This yolk-shell Si@C@void@C material displayed superior cycling stability and rate performance compared to Si@C and Si@void@C. The Si@C showed an initial charge capacity of 1479 mAh/g which rapidly decayed to 552 mAh/g after 50 cycles. Meanwhile, the Si@void@C presented a slightly decreased initial charge capacity of 1132 mAh/g, but enhanced capacity retention of 66% after 50 cycles. In sharp contrast, the initial charge capacity of Si@C@void@C was as high as 1910 mAh/g and retained 71% of the initial capacity after 50 cycles (Fig. 3h). In addition, the capacity of Si@C and Si@void@C attained at the current density of 4 A/g were approximately 10% and 41% of that at 100 mA/g, respectively, while Si@C@void@C was up to 60% (Fig. 3i). An extended study to form silicon/double-shells yolk-shell nanostructure was explored lately. Sun et al. [25] prepared Si@void@C@void@C structure still using SiO₂ as sacrificial layer. The presence of double carbon shells greatly improved electronic conductivity. This dual yolk-shell material maintained a capacity as high as 943.8 mAh/g at 50 mA/g over 80 cycles. Yang et al. [26] also prepared dual yolk-shell Si@void@SiO2@void@C structure through selective etch SiO₂ templates. The SiO₂ and C dual shells provided a double barrier to accommodate huge volumetric variation of Si during lithiation and protected Si NPs from electrolyte corrosion. The Si@void@SiO2@void@C displayed stable capacity of 956 mAh/g after 430 cycles at 0.46 A/g with capacity retention of 83%. Even at a high current density of 5.8 A/g, the specific capacity of the dual yolk-shell structure was stabilized around 250 mAh/g. When the current density returned to 0.46 A/g, the specific capacity recovered to about 1000 mAh/g, indicating good stability of such dual yolk-shell silicon-based structures.

The synthetic methods as mentioned above are commonly adopting SiO₂ as sacrifice layer and are inevitable to involve HF solution which is difficult to realize commercial production because of its toxic and environmental problems. A few researchers employ other facile routes to synthesize yolk–shell Si@void@C structures by replacing the SiO₂ layer by other coatings, in order to substitute HF etching by some other eco-friendly solutions. Su et al. [27] prepared Si@void@C nanocomposites via a facile method of resorcinol–formaldehyde (RF) coating and LiOH etching. The size of Si cores (50–100 nm) and voids could be controlled by optimizing the etching times. The Si@void@C composites presented considerable reversible capacity of 628 mAh/g after 100 cycles and good rate performances.

Ma et al. [28] prepared Si@void@C structures by depositing MgO as intermediate layer. It started with the surface oxidation of Si using aqueous ammonia, followed by the addition of MgSO $_4$ and Na $_2$ CO $_3$ leading to the formation a Si@SiO $_2$ @MgCO $_3$ precursor by a precipitating process. Subsequently, Mg $_2$ SiO $_4$ @MgO@C shell was obtained by a calcining and CVD method. After removing

the interlayer by magnesiothermic reduction and HCl etching, the Si@void@C yolk-shell structure was formed finally (Fig. 4). Here, the amount of MgO coating was investigated and the proper mass ratio of MgO and Si was about 2. Such Si@void@C anode exhibited a reversible charge capacity of 901 mAh/g at the first cycle and a capacity of 796 mAh/g after 100 cycles at 1.0 A/g with the capacity retention of 88.3%. Moreover, the nanocomposite exhibited good rate capacity, retaining 350 mAh/g at a current density of 5.0 A/g.

Accordingly, the yolk-shell structure can significantly improve the cycling stability of Si-based composites with low areal mass loading ($\leq 0.2 \,\mathrm{mg/cm^2}$). However, its intrinsic large specific surface area and hollow space would decrease the tap/packing density of the electrode inevitably, which leads to a low volumetric capacity and limits its practical applications in LIBs. To tackle this problem, advanced version of micrometer-sized particle with yolk-shell NPs are designed and prepared in terms of areal mass loading and material tap-density (related to volumetric capacity). Liu et al. [29] fabricated Si@void@C volk-shell composite based on a novel pomegranate-inspired design. The void space of such hierarchical structure could accommodate the expansion/contraction of Si NPs. The integrity of the composite by interconnected carbon shells could increase the electrical contact of the individual NPs and decrease the contact area to the electrolyte. Therefore, such hierarchical microparticle displayed a high capacity of above 1160 mAh/g after 1000 cycles at C/2 with excellent cycling stability (0.003% decay per cycle) and an average coulombic efficiency of 99.87% in 500-1000 cycles. Impressively, the microparticle possessed a higher tap density of 0.53 g/cm³ than the original Si NPs (0.15 g/cm³). Thus, the microparticle electrode with 3.12 mg/cm² mass loading exhibited high areal capacities of \sim 3.1 mAh/cm² (gravimetric capacity: 950 mAh/g) after 200 cycles at 0.7 mA/cm², which was comparable to commercial graphite. Besides, Lin et al. [30] prepared Si@void@C composite by a new method, which started with mechanical pressing of silica-coated Si NPs to pellets (Si@SiO2), Si@SiO2 power in micrometer-size was then obtained by subjecting to thermal sintering at 600 °C for 2h to link nanoparticles together, followed by coating with carbon to form Si@SiO2@C particles with an average diameter of \sim 4.4 µm in size. Finally, the SiO₂ was etching to provide enough empty spaces for Si volume change. The tap density of these micrometer-sized particles was 0.91 g/cm³, which was about twice as high as the value of above Si/C micrometer. The resulted anodes with a high mass loading of 2.02 mg/cm³ exhibited a high areal capacity of \sim 3.5 mAh/cm² (1733 mAh/g) at 0.1 mA/cm². It was concluded that the electrodes based on such special form possessed both high mass loadings (high tap/packing density) and good cycling stability (effective alleviation of the volume change), which well combined the advantages of both bulk and nanoscale.

2.3. Porous structure

The principles of adopting porous structure designs to improve the performance of Si/C anodes are similar to those of yolk–shell structures, that is, the introduced void space provides adequate room for volume expansion of Si during Li–Si alloying process, correspondingly minimizing the loss of particle contact and alleviating the stresses. The electrodes based on the engineered porous Si/C composites possess extraordinary stable structure during cycling. In addition, large surface area and uniformly distributed channels short the diffusion path for Li ions and increase reactivity of the composites, thus leading to enhanced rate capability. These Si/C composites have a significant potential for rapid charging in LIBs. The porous Si/C structures usually include two types: (1) porous silicon matrix is coated by carbon layers, denoted as p-Si/C; (2) Si NPs are dispersed in porous carbon matrix, denoted as Si/p-C. At present, p-Si/C structure is commonly synthesized from silica

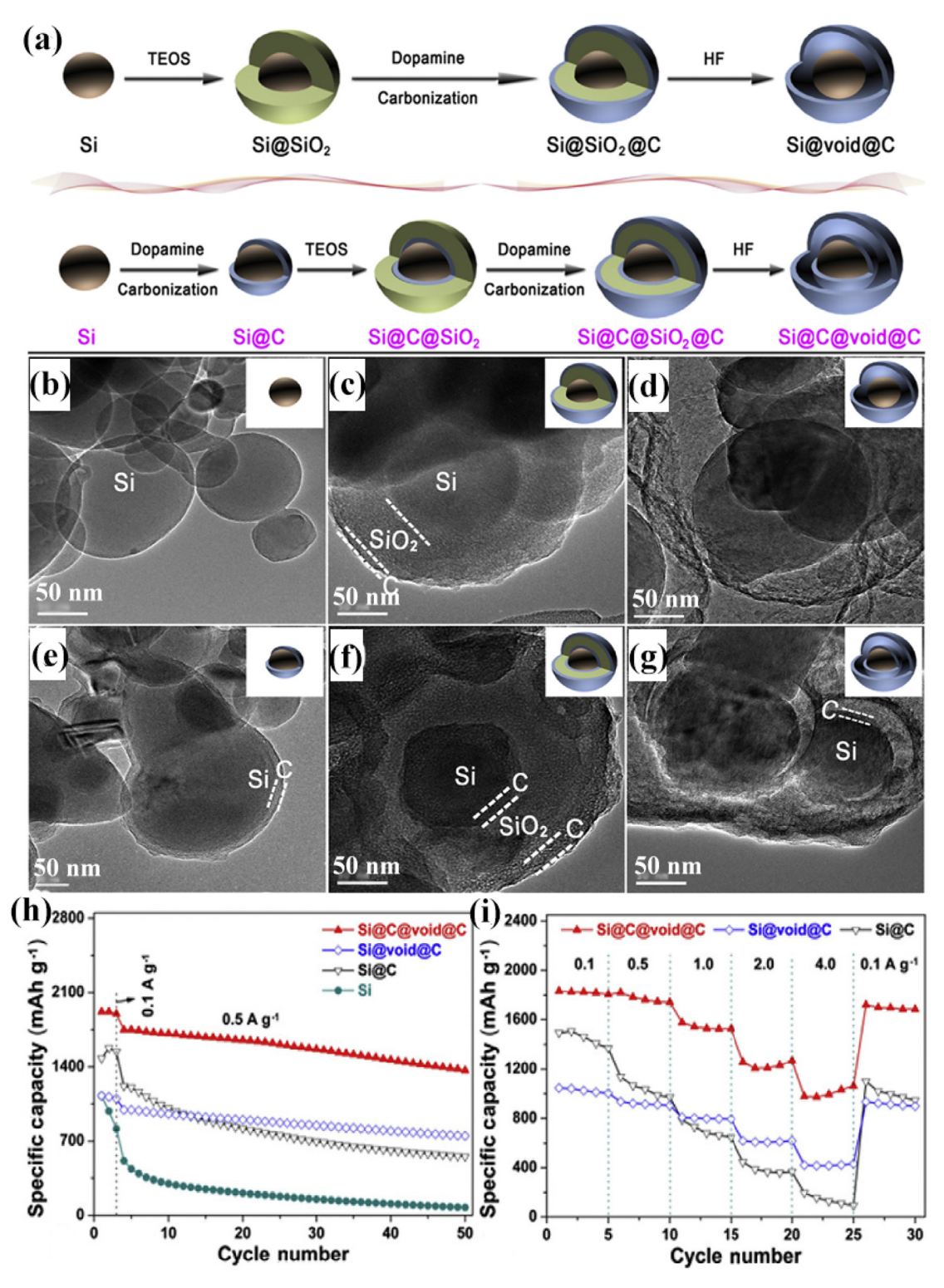


Fig. 3. (a) Schematic diagram of the formation process of traditional yolk–shell Si@void@C and novel core–shell yolk–shell Si@C@void@C; (b) TEM images of raw Si, (c) Si@SiO₂@C, (d) Si@void@C, (e) Si@CG, (f) Si@CG, and (g) Si@C@void@C; (h) Cycling performances of Si, Si@C, Si@void@C, and Si@C@void@C electrodes at 500 mAg/g; (i) Rate performances of Si@C, Si@void@C, and Si@C@void@C electrodes at specific current from 100 to 4000 mAg/g. Reprinted with permission from Ref. [24]. Copyright (2015) Published by Elsevier Ltd.

through magnesiothermic reduction [31–36], which is amenable to scale-up.

Wang et al. [31] synthesized porous Si/C composites from diatomite as a raw material through a magnesiothermic reduction process, followed by impregnation and carbonization of phenolic resin. The effect of different ratios of Si and C was investi-

gated, and it was found that the porous Si/C composite containing 33% carbon exhibited the highest initial reversible capacity of around 1628 mAh/g with superior capacity retention. With the current density increased to 2000 mA/g, the reversible capacity was still maintained at 776 mAh/g. The enhanced performance was attributed to the rich porous channels and the good carbon conduc-

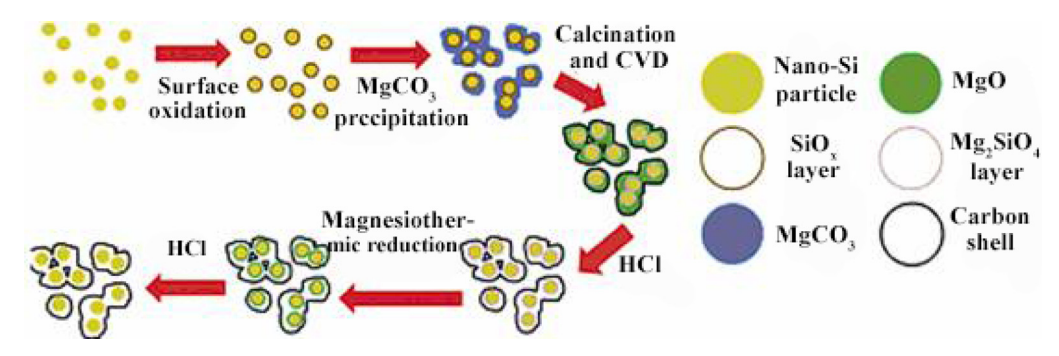


Fig. 4. Schematic illustration of the formation process of yolk-shell structured Si/C nanocomposite. Reprinted with permission from Ref. [28]. Copyright(2017) Elsevier B.V. All rights reserved.

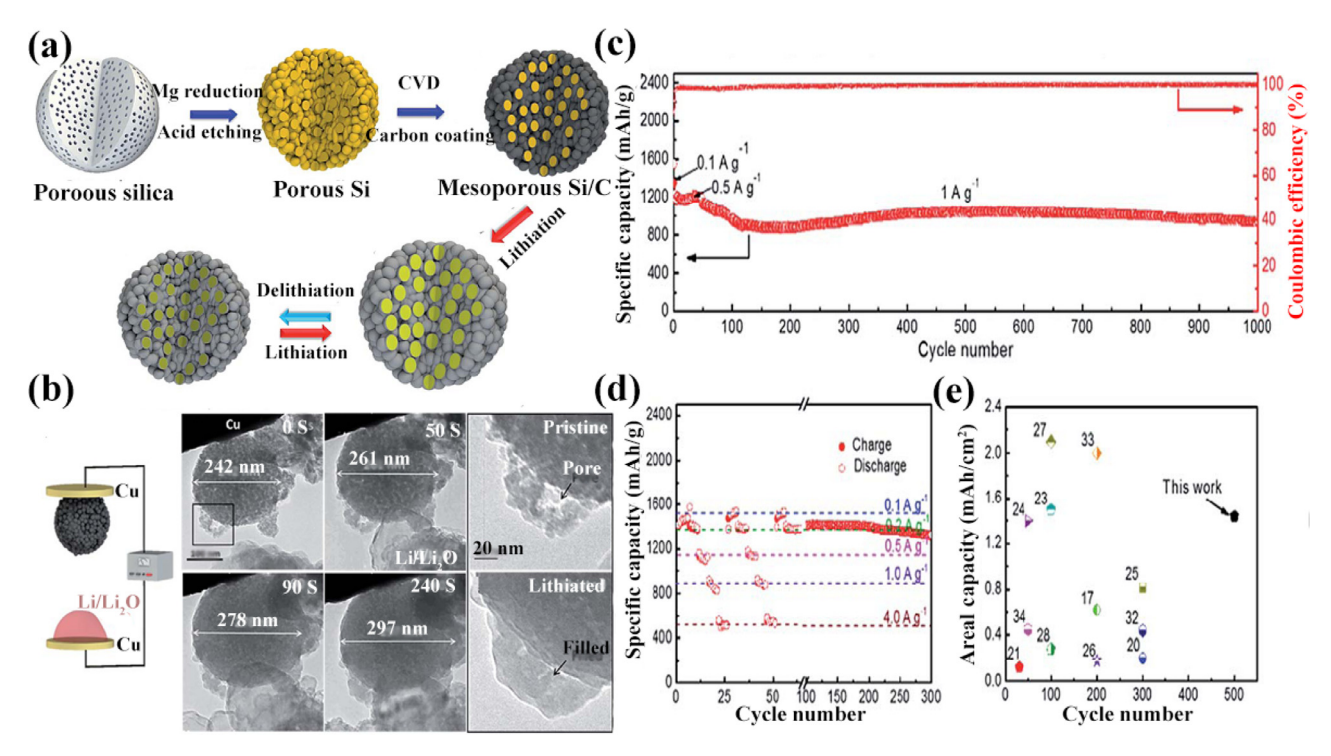


Fig. 5. (a) Schematic diagram for the synthetic procedure of the mesoporous Si/C microspheres; (b) In situ TEM examination of the lithiation process of a mesoporous Si/C microsphere; (c) Cyclic performance for 1000 cycles at 1 A/g after activation at 0.1 and 0.5 A/g for 50 cycles; (d) Rate capability measured at different current densities in the range of 0.1–4.0 A/g; (e) Plot of cycle number versus areal capacity for different Si/C-based electrodes with reference numbers next to the corresponding data. Reprinted with permission from Ref. [36]. Copyright (2016) Royal Society of Chemistry.

tive network, which accommodated large volume expansion of Si without fracturing the SEI at the outer surface during cycling and improved the composite electrical conductivity, respectively. Li et al. [32] constructed 3D interconnected porous Si/C architectures via a controllable magnesiothermic reduction route from silica aerogels. The Si nanocrystals grew into Si nanosheets and assembled into 3D interconnected hierarchically porous Si architectures. The anodes exhibited improved reversible capacity of 1552 mAh/g after 200 cycles at 200 mA/g and good rate capacity of 1057 mAh/g at a current density of 2.0 A/g even after 50 cycles.

An outstanding study about porous Si/C structures was conducted by Xu et al. [36], who prepared mesoporous Si/C microspheres of $\sim 165\,\mathrm{nm}$ diameter by magnesiothermic reduction of porous silica followed coating of a thin carbon layer by CVD method. Numerous ultrafine primary Si nanocrystals of $\sim 10\,\mathrm{nm}$ diameter were surrounded by clearly defined internal pores based on TEM images (Fig. 5a and b). The carbon coating formed over the whole Si/C microsphere was very uniform. Therefore, excellent high specific capacity and cycling stability were achieved. The Si/C

electrodes delivered a reversible capacity of ~1500 mAh/g at 0.1 A/g. The capacity retention was up to $\sim 90\%$ (~ 990 mAh/g) after 1000 cycles even at 1.0 A/g (Fig. 5c). In addition, an outstanding areal capacity of ~1.44 mAh/cm² after 500 cycles was obtained (Fig. 5d). In situ TEM has been employed to observe the lithiation/delithiation processes, in which a highly reduced volume expansion of ~85% upon full lithiation was measured and calculated (Fig. 5b). The result was much less than the theoretical prediction of ~300% for solid Si particles. This study clearly revealed that well-engineered porous Si/C structures possessed the potential to serve as anodes for the next-generation LIBs (Fig. 5e). A new type of porous Si@C coaxial nanotubes was fabricated by Chen et al. [34]. Firstly, ZnO nanorods were synthesized by a seed-assisted method. Afterward, the ZnO nanorod template was deposited with SiO₂ and carbon layers, successively. Followed by magnesiothermic reaction, the SiO₂ layer converted into a porous Si layer, resulting in the formation of porous Si@C coaxial nanotubes. The coaxial nanotubular structures could provide enough space to alleviate the large volume expansion and more reaction sites for lithium alloying reactions. Meanwhile, the carbon layer could improve electronic conductivity and stabilize nanotubular structure and the interface silicon-electrolyte during the lithiation/delithiation process. The porous Si@C coaxial nanotubes delivered a superior cycling performance of $\sim\!1300$ mAh/g after 200 cycles at $200\,\text{mA/g}$ in the VC-containing electrolyte and a high coulombic efficiency of over 98% after the first cycle.

Synthesis of p-Si/C from cheap source with scalable methods has been one of the major issues in this time range. Besides the above mentioned magnesiothermic reaction, many researchers are always exploring other simple, low-cost and saleable routes to synthesize p-Si/C structure. Zhang et al. [37] applied Rochow reaction to realize a scalable synthesis of porous Si/C composites. The starting materials were commercial Si microparticles which reacted with gas CH₃Cl over various Cu-based catalyst particles. Substantially, the macropores were created within the unreacted Si along with carbon deposition to form porous Si/C composites. The porous Si/C electrodes showed the first charge capacities of 856.5 mAh/g. The reversible capacity retained at 732.1 mAh/g after 100 cycles with an average rate of around 0.15% cycle. The enhanced performance was attributed to the interconnected porous structure and conductive carbon-coated layer. It is believed that the production of porous Si/C anodes on industrial scale was highly possible by combining the organosilane synthesis process and controlling reaction conditions. Tian et al. [38] developed a novel method to produce porous Si/C anodes from the abundant and low cost Al-Si alloy ingot. The method consisted of acid etching, ball-milling and carbonization procedure to yield the unique micro-sized (2-10 μm) nano-porous Si/C composites, which were composed of 20 nm carbon coating and 200 nm nano-Si cluster derived from ~20 nm Si particles. The hierarchical porous structure with carbon coating could stabilize the SEI layer and the inside nano-scaled pore, so as to offer adequate room for volume expansion as well as relax the stress/strain. The nano-porous Si/C anodes exhibited high overall capacity of 815 mAh/g at a current density of 500 mA/g, and maintained 86.8% of initial capacity after 300 cycles, with an average loss of only 0.044% per cycle.

As for Si/p-C composites, multiple methods have been investigated to create various Si/p-C structures which also possess significantly improved electrochemical performance. Liu et al. [39] used commercial nano-CaCO₃ as template for the preparation of porous carbon substrate, followed by chemical vapor deposition of Si NPs onto the surface of porous carbon substrate to form porous Si/C structures. The carbon substrate acted as both supporter for accommodation of Si expansion and barrier to prevent the internal silicon particles from being exposed to electrolyte. The electrode maintained superior structure stability after 200 cycles with a specific capacity of over 850 mAh/g and a coulombic efficiency of 99.5% at 500 mA/g.

Ma et al. [40] prepared SiO₂-CTAB@polymer microspheres through hydrolysis and condensation of TEOS and a polymer of resorcinol-formaldehyde. Subsequent carbonization and magnesiothermic reduction were executed to generate mesoporous Si@C microspheres (Fig. 6a). The Si@C microspheres had regular spherical shapes with a mean diameter of around 500 nm and a mesopore size of 3.2 nm (Fig. 6b and c). This material exhibited good electrochemical reversibility and structural integrity. A specific capacity of 1375 mAh/g at 50 mA/g was delivered, and the charge capacity still remained 1054 mAh/g after 100 cycles with high coulombic efficiency of 98% (Fig. 6d). Besides, the composite exhibited good rate capacity, retaining 628 mAh/g at current density of 2.0 A/g (Fig. 6e). The good electrochemical performance resulted from the mesoporous voids between Si NPs and the carbon framework, which afforded a medium for tolerating the volume variation of Si NPs and therefore kept electrode integrity during the lithiation/delithiation process. Song et al. [41] also fabricated porous cage-like carbon/nano-Si composites based on nano-Si@zeolitic imidazolate frameworks-templated method. The obtained porous Si/C composite demonstrated a high reversible capacity (\sim 1168 mAh/g at 100 mA/g after 100 cycles), improved cycling stability, and excellent rate capacity.

Despite the Si/p-C electrodes possess promising performance, their use for Li-ion batteries suffers from complex and limited synthetic routes for their preparation. To tackle such issues, Sohn et al. [42] proposed a scalable and nontoxic method to synthesize porous Si/C composites with the aid of chemical etching Si and carbon phases using alkaline solution (Fig. 7). Firstly, commercially available bulk Si powder was ball-milled and mixed with pitch. After a carbonization and subsequently etching reaction via NaOH solution, porous Si/C structure was received. The obtained porous Si/C electrode displayed an expansion of the height by ~22% after the first lithiation and only 16% after the first cycle. A reversible capacity of 1077 mAh/g was obtained and the coulombic efficiency of the porous Si/C electrode was more than 98% during most cycles, while the coulombic efficiency of non-porous Si-C electrode was less than 95%.

Most of the aforementioned porous Si/C composites display a large size in nanoscale, however, larger-sized porous Si/C composites are needed and designed to increase the tap/packing density, which offers an important guidance principle to fabricate high-performance Si anodes with high mass loading. Such microsized porous structures are composed of ultrafine nanostructures with nano-sized carbon coating shell, pores in nano-size and Si nano-particles, which can effectively improve the cycling performance (by accommodating the volume change of Si upon cycling) and areal/gravimetric/volumetric capacities (by the tap/packing density) of the anodes. Wang and co-workers [43] fabricated carbon-coated porous Si micro-particles by a simple method, which consisted of a sol-gel and thermal disproportionation reaction to form a Si NP-interconnected porous structure and further carbon coating process. This electrode with a tap density of 0.68 g/cm³ displayed higher capacities (1600 mAh/g and 1088 mAh/cm³ after 150 cycles at 400 mA/g) than both Si NPs (1200 m Ah/g and 192 mAh/cm³, 0.16 g/cm³ tap density) and graphite (370 mAh/g and 429 mAh/cm³, 1.16 g/cm³ tap density) [7]. Lu et al. [44] prepared micro-sized nonfilling carbon-coated porous Si particles by heating commercially SiO microparticles after resin coating. Such structure was composed of the inner porous microsized core (interconnected Si NPs) and the outer carbon coating shell, which was different from other carbon-coated porous Si structures with carbon coating shell penetrating into the interior Si surfaces. The porous core accommodated the volume variation of Si, while the carbon shell prevented the formation of unstable SEI layer and increased the electrical conductivity. Therefore, the electrode with a high mass loading of 2.01 mg/cm² exhibited a high areal capacity of 2.84 mAh/cm² (1413 mAh/g, 789 mAh/cm³) after 100 cycles at a current density of 0.25 mA/cm² (500 mA/g), which was comparable to a commercial LIB cell.

2.4. SiO_x/C type

As a form of silicon-based anode, SiO_x (0 < x < 2) is considered to be very attractive material due to its high specific capacity (\sim 1600 mAh/g), low charge–discharge potential and lower volume expansion than Si. Such structure of SiO_x consisted of nano-Si (2–5 nm) homogeneously distributed in a matrix of SiO_2 with glass-like structure. The relative excellent cycle performance of SiO_x anode is related to the high strength of Si–O bond (twice as strong as Si–Si bond) as well as the formation of lithium silicates and Li_2O , which alleviate the effects of volume expansion. Nonetheless, the electrical conductivity and rate capability of SiO_x remain quite poor due to the transformation of low-conductivity

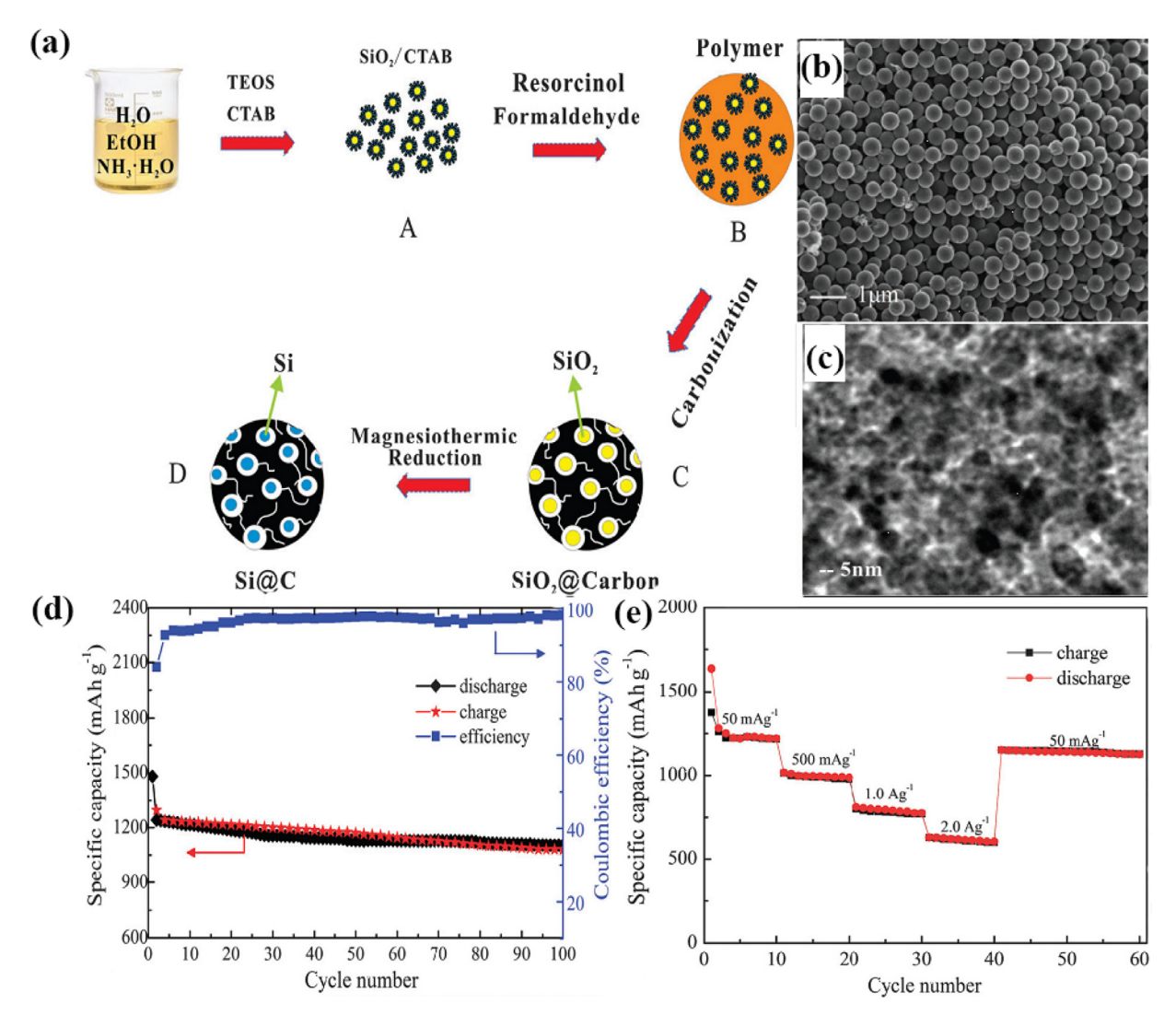


Fig. 6. (a) The schematic fabrication process of mesoporous Si@C microspheres; (b) SEM and (c) TEM images of Si@C-MII microspheres; (d) Specific discharge-charge capacity and coulombic efficiency of the Si@C-MII anode at 50 mA/g after 100 cycles; (e) Discharge-charge performance of mesoporous Si@C-MII anodes at various current densities. Reprinted with permission from Ref. [40]. Copyright (2013) Royal Society of Chemistry.

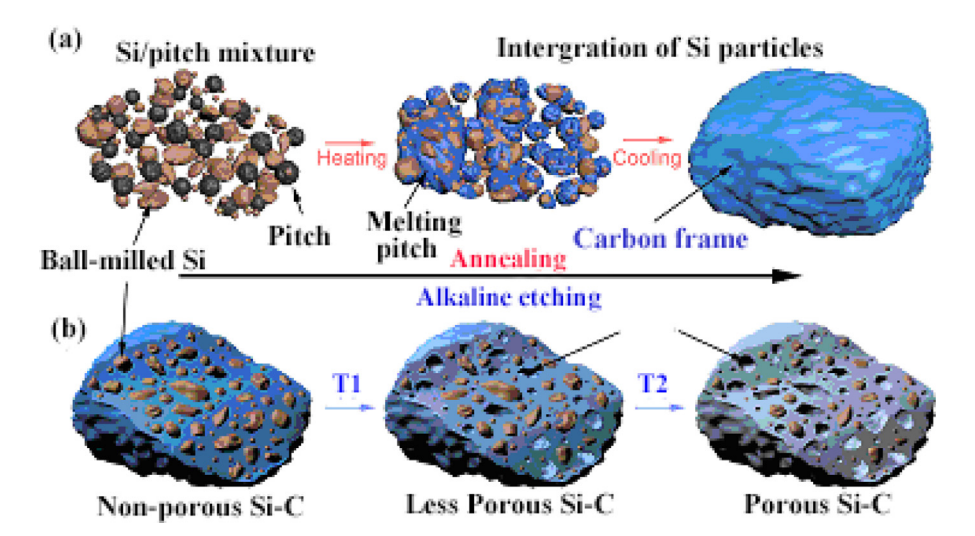


Fig. 7. (a) Schematic illustration of fabricating non-porous Si–C composite by annealing method and (b) porous Si–C composite by etching non-porous Si–C in alkaline solution. Reprinted with permission from Ref. [42]. Copyright (2016) Elsevier Ltd. All rights reserved.

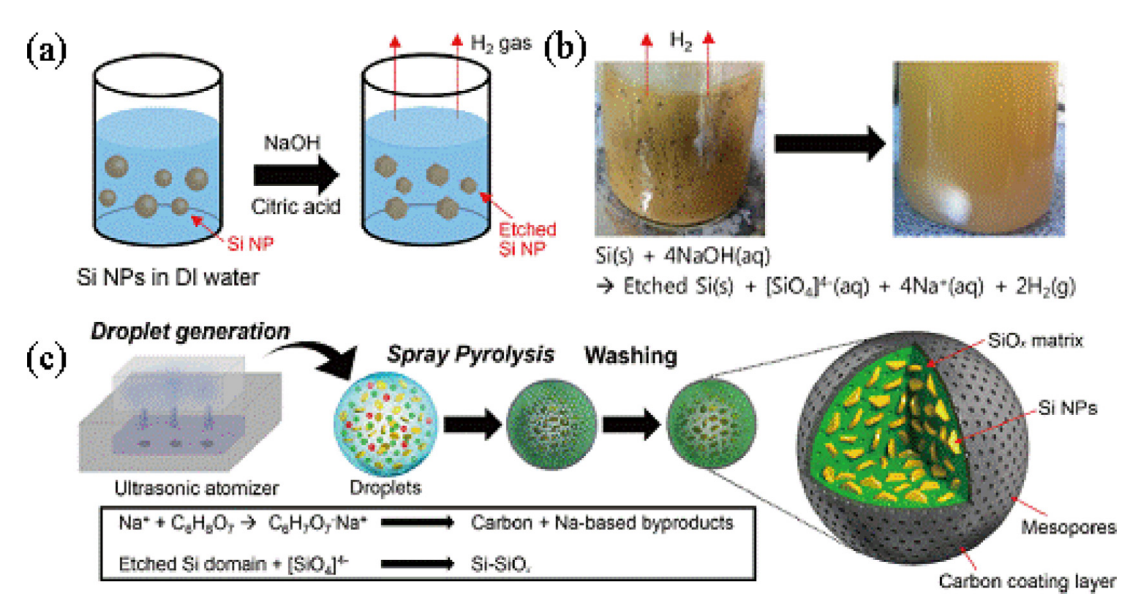


Fig. 8. Synthesis of the Si–SiO_x@C composite via one-step spray pyrolysis method. Reprinted with permission from Ref. [46]. Copyright (2017) American Chemical Society.

and high-stiffness Li₂O layer and its inevitable volume expansion during charge/discharge cycles. Thus, the rational design strategies discussed above for Si should be applicable to address the issues of SiO_x. Among all these methods, carbon coating is acceptable in view of low cost and better cyclic performance for practical application. A few researchers have proposed facile synthetic methods to prepare such $SiO_x@C$ composites. Wang et al. [10] prepared core-shell structured Si-SiO_x@C particles by ball-milling crystal micron silicon and citric acid powders under Ar atmosphere followed carbonization. The composite offered a specific capacity of 1450 mAh/g after 100 cycles at 100 mA/g. Even at a current density of 500 mA/g, the specific capacity still maintained at 1230 mAh/g after 100 cycles. Jiang et al. [45] developed a different method to synthesize Si-SiO_x@C composite by direct pyrolysis of poly(methyl methacrylate) (PMMA) polymer onto the surface of Si powder. The PMMA thermally decomposed with their alkyl chains converting to carbon while its residue oxygen which recombined with Si to form SiO_x. The obtained nanocomposite revealed a high charge capacity of 1972 mAh/g and discharge capacity of 2560 mAh/g in the first cycle. Stable cycling with a capacity retention of more than 1030 mAh/g over 500 cycles and high coulombic efficiency of above 99.5% at 0.5 A/g were delivered, exhibiting a great promise for practical applications.

Lee et al. [46] have constructed Si-SiO_x@C composite, where Si nanodomains were homogeneously embedded in the SiO_x matrix with a carbon surface layer. The process started from mixing Si NPs, citric acid, and sodium hydroxide into distilled water, in which Si NPs were etched by NaOH with the production of SiO₄^{4–}. With the aid of a spray pyrolysis machine, SiO₄^{4–} transformed to SiO_x matrix and citric acid decomposed to carbon layer (Fig. 8). The composite exhibited outstanding electrochemical performance, a reversible capacity of 1561.9 mAh/g at 0.06 C rate with initial coulombic efficiency of 80.2% and a capacity retention of 87.9% at 1 C rate after 100 cycles.

In industry, SiO_X has attracted much attention worldwide, Samsung SDI, Sumitomo Titanium Corp, BTR and LG Chem have devoted tremendous efforts to carry out SiO_X/C commercialization research. Therein, the SiO_X produced by Shinetsu Co. have already been practically used in small batch with a low weight ratio mixed with graphite, while BTR New Energy Materials Inc. also supplied SiO_X/C commercial products for Li-ion batteries. Although SiO_X/C anodes have been used in real LIBs, there is still a certain gap for really practical application of SiO_X/C on account of its low initial

coulombic efficiency because of the irreversible electrochemical reaction between ${\rm Li}^+$ and ${\rm SiO_2}$ matrix in the first cycle. The resulted large irreversible capacity of the anode will no doubt consume a lot of lithium from cathode and correspondingly decrease the energy density of the full lithium ion batteries. In order to increase the first cycle efficiency, the technique of prelithiation treatment is developed which will be described in detail in the following section.

2.5. Embedding type

The embedding type Si/C composites mean that silicon is embedded in a continuous carbon matrix. It has been found that composting silicon with different carbonaceous matrixes as buffer medium can effectively improve the cyclability of Si-based anode by accommodating volume variation and releasing mechanical stress of silicon during lithiation/delithiation cycles. Particularly, carbonaceous materials such as graphite, carbon nanotubes/nanofibers and graphene, have been widely exploited as matrixes.

2.5.1. Graphite

Using graphite composited with Si particles has been regarded as an effective strategy to improve the electrochemical performance of Si-based anode. The final composite material consists of Si particles intercalated between the lamellar structure of graphite flakes, where the graphite can not only serve as effective substrates to stabilize the SEI layers but also prevent the aggregation of Si particles and promote electronic transport of the anode [47]. However, the choice of compositing methods is quite limited at the early stage, and Si/graphite composites are mainly prepared by directly milling the mixture of Si and graphite powders. Kim [48] used a unique high energy milling process to prepare nano-Si/graphite composite. The structure with nanometer Si powder dispersed in graphite matrix was designed, with the purpose of alleviating the volume change of Si and hindering the reaction between Si and electrolyte during charge-discharge. Compared to pure nano-Si, the Si/graphite composite displayed better cyclability, its capacity retention ratio was near 90% after 15 cycles. The total capacity fade of nano-Si/graphite was only 40 mAh/g between the first and the fifth cycle, which was less than that of nano-Si (the capacity fade was 125 mAh/g). Particularly, the author pointed out that the use of nano-sized Si particles also played an important role in the improvement of the cyclic stability due to their good plasticity and deformability. Besides direct milling method, Holzapfel et al. [49] prepared Si NPs/graphite composite via thermal vapor deposition of Si onto the surface of fine graphite particle. The Si/graphite composite with 20% of Si displayed an initial capacity of 1350 mAh/g, while the discharge capacity for the following 100 cycles was maintained about 1000 mAh/g at 74 mA/g. The relatively slow capacity loss upon cycling was mainly attributed to homogeneous distribution and good adherence of the Si NPs on the graphite surface. Moreover, the role played by the graphite matrix here was controlling the expansion of Si particles, therefore increasing mechanical stability of the Si-anode.

However, as for Si/graphite composite, only a limited improvement of cyclability can be obtained originated from the decrease of volume changes for embedded Si particles. That cannot meet the practical battery requirements due to the deterioration of the Si/graphite based anodes during cycling. Such results may arise from the loose connections among flaked graphite particles and the poor interface adhesion between graphite and Si, which do not allow a complete control of the volume changes. In order to achieve high capacity over graphite and good cyclability for the Si/graphite composite, it is of paramount importance to construct multicomponent systems by introducing another internal organic carbon source. On one hand, the addition of organic polymer within such Si/graphite composite is beneficial for forming strong interface bonding between the graphite and Si, and enables a uniform distribution of Si particles on graphite. On the other hand, a unique kind of structure, originated from the introducing organic carbon sources, can be constructed and applied as buffer medium to stabilize the Si electrodes. Datta and Kumta [50] synthesized a novel kind of Si/graphite/PAN-C composite by distributing active Si phase in graphite matrix and then coating with thermally decomposed product polyacrylonitrile (PAN)-based amorphous carbon (PAN-C). The presence of PAN acted as a diffusion barrier to inhibit the interfacial diffusion reaction between graphite and Si and thus the graphite retained its desired graphitic structure. Such intact graphite together with the PAN-C severed as ductile carbonaceous matrix to relieve the volume change of Si and suppressed the irreversible loss of the anode. The resultant composites exhibited a reversible capacity of 660 mAh/g with almost no decay up to 30 cycles at a constant current of 160 mA/g $(\sim C/4)$. Lee et al. [51] also synthesized a spherical nanostructured Si/graphite/carbon composite by pelletizing a mixture of Si NPs, graphite and petroleum pitch powders, followed by heat treatment at 1000 °C under an argon atmosphere. The composite material exhibited good electrochemical properties including a high reversible specific capacity of ~700 mAh/g, high coulombic efficiency of 86% in the first cycle, and good capacity retention. That was attributed to the enhanced structural stability of the composite, in which the mechanical stress induced by the volume change of nano-Si during cycling was effectively buffered.

Wang et al. [52] successfully synthesized Si@flake-graphite/amorphous-carbon (Si@FG/C) microspheres with a porous spherical shape via a combined ball-milling and spray drying method (Fig. 9a). Commercial Si NPs and flake-like graphite were sufficiently mixed by dry ball milling. Afterward, Si@FG/C porous microspheres were obtained with a spray drying process followed by high temperature heating, where glucose and polyvinylpyrrolidone (PVP) were used as binder to combine Si and graphite and then as carbon source to coat Si and graphite. This Si@FG/C composites with unique structure displayed good cycle life and rate capability. A capacity retention of 90% (over 400 mAh/g) was achieved over 300 cycles at 500 mA/g (Fig. 9b), while a capacity of 200 mAh/g was obtained at a high current density of 5 A/g (Fig. 9c). Herein, the binding effect of glucose and PVP as well as the resultant amorphous carbon were responsible for the formation of

such porous spherical structure, which was critical for the excellent cycle stability. The amorphous carbon absorbed mechanical strain from the volume expansion of Si while the porous structure buffered the volume change of Si during cycling. The effective conductive networks built by FG and amorphous carbon accounted for the good rate capability of the composites. Besides, the small size of Si NPs was also favorable for good rate capability of the composites.

The above studies suggest that the Si/C composites based on Si, graphite and mesophase organic pyrolytic carbon have been successful in extending the cycle life and rate performance of Si. Besides, the easy preparation, low cost, and relative good electrochemical performance make such Si/graphite/pyrolytic carbon composites promising to serve as appropriate anodes for high-performance LIBs.

2.5.2. CNTs/CNFs

Apart from graphite particles, one-dimensional (1D) carbon nanotubes (CNTs) and carbon nanofibers (CNFs) are also alternative materials to composite with Si. Compared with graphite, CNTs and CNFs have excellent electrical conductivity, superior mechanical strength and large aspect ratio, which enable better electric conductivity and higher degree of resiliency [53,54]. As a result, CNTs and CNFs are more effective to construct conductive network and better suitable ductile host matrix to alleviate the adverse effect induced by volume changes of Si anodes. Zhang et al. [55] produced Si/C composite which was made of carboncoated Si NPs (Si@C) interweaved with CNTs and CNFs, denoted as Si@C/CNTs&CNFs. The synthesis procedure started with mixing nano-Si with citric acid in a nickel acetate-ethanol solution. Then, Si@C particles were generated by spray drying and heating the obtained dispersion under N₂ atmosphere. The resulting Si@C particles with nickel oxide dispersed on their surfaces, which acted as a catalytic agent, were finally subjected to a C₂H₂/N₂ treatment at 700 °C to form the Si@C/CNT&CNF composite. The Si@C/CNTs&CNF composite exhibited high capacities with superior cycling stability (1195 mAh/g after 50 cycles at 300 mA/g). In contrast, Si@C without CNTs and CNFs displayed insufficient capacity retention (only 601 mAh/g after 50 cycles), whereas Si NPs without carbon coating had the worst performance with its capacity dropping to nearly zero after 15 cycles. The superior performance of Si@C compared to that of Si NPs was in good accordance with studies discussed in Section 2.1. As for the Si@C/CNT&CNF composite, the CNTs and CNFs provided continuous electronic pathways by linking most of the Si@C particles together and offered void space (interweaved with Si@C particles) to absorb the volume expansion of Si, thereby decreased the breakage of the conduction network during cycles and thus displayed superior cycling stability. Besides, the in situ growth of CNTs by CVD method has often been exploited to prepare Si/CNT composite. Kim et al. [54] used CVD method to grow CNTs directly onto the surface of fine Si NPs to prepare Si/CNTs composite. The performance of the electrode was superior to that of bare Si and Si-CNTs directly mixed electrodes. It was supposed that the void space and the flexible characteristics of the CNTs accommodated the volume expansion of Si core without severe electrode swelling. Another interesting concept was realized by Wang and Kumta [56], where a simple twostep CVD method was applied to build vertically aligned multiwall CNTs on quartz slides with xylene as the carbon source and ferrocene as the catalyst. Si NPs were deposited onto CNTs by using SiH₄ as Si source with clearly defined spacing. This novel structure maintained a stable reversible capacity of ~2050 mAh/g after 25 cycles with little loss of 0.15% per cycle. Increasing the current rate to 2.5 C, a capacity of ~1000 mAh/g was achieved, indicating high rate capability. Similarly, Gohier et al. [57] investigated the electrochemical characterization of Si NPs decorated ver-

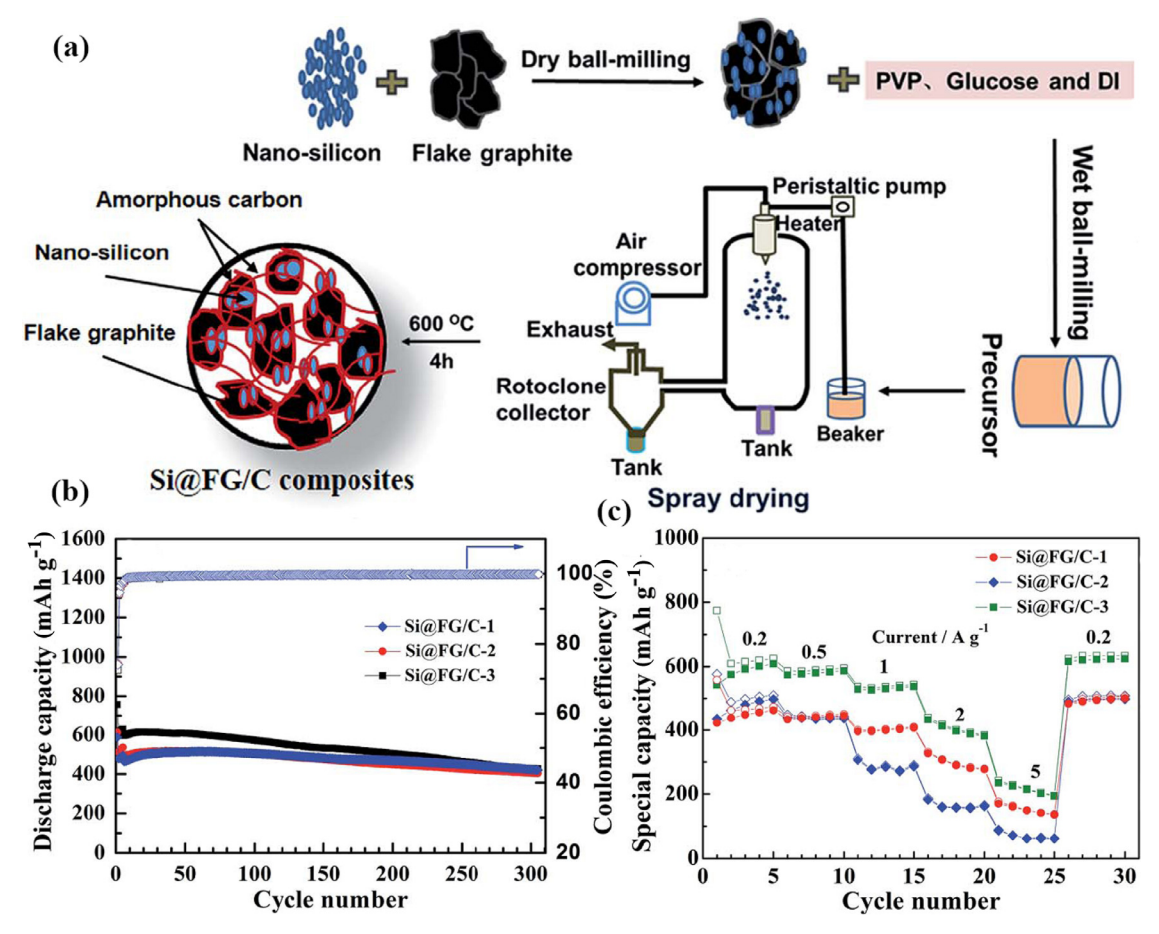


Fig. 9. (a) Schematic illustration of the Si@FG/C composite preparation process; (b) Cycle performance, coulombic efficiency and (c) rate capabilities at various rates for the Si@FG/C composites electrodes. Reprinted with permission from Ref. [52]. Copyright (2016) Royal Society of Chemistry.

tically aligned CNTs, which were directly grown onto metal foil via a two-step CVD process. This specific hierarchical hybrid nanostructure was made of very thin CNTs (5 nm in diameter) on which Si NPs (10 nm) were homogeneously deposited. Such Si/CNTs exhibited high reversible capacity of 3000 mAh/g at 1.3 C and an impressive rate capability (a capacity of 1900 mAh/g at 5 C and 760 mAh/g at 15 C). Such excellent electrochemical performance originated from the perfect adhesion between CNTs and Si NPs, which facilitated electron and Li⁺ transport and limited the diffusion process occurring in conventional graphite-based electrodes. Besides, the superior flexibility of CNTs was also favorable to accommodate the severe volume change and absorb the mechanical stress of Si upon Li⁺ intercalation/de-intercalation process. Recently, Mangolini [58] proposed a novel approach based on a liquid dispersion comprising of Si quantum dots, CNTs and polyvinylpyrrolidone (PVP). Coating the suspension onto copper foil was followed by appropriate annealing cycles under inert atmosphere, leading to the formation of a well-dispersed heterojunction of Si NPs and CNTs. This composite possessed a capacity of approximately 1000 mAh/g for 200 cycles with a coulombic efficiency of 99.8%.

Encapsulation of Si NPs into CNFs has also been regards as an efficient approach to improve the electrochemical performance of Si anode. And electrospinning offers a low cost and scalable technique to fabricate Si NPs/CNFs composites. Hwang et al. [59] fabricated peculiar Si NPs/CNFs fibers by an electrospinning process using a dual nozzle (Fig. 10a). In this process, Si NPs and poly(methyl methacrylate) dissolved in *N*,*N*-dimethylformamide (DMF) and acetone was injected into the core channel of the nozzle. Polyacrylonitrile (PAN) dissolved in DMF was injected into the shell channel of the nozzle. Then, the electrospinning process was conducted

and the final Si NPs/CNFs composite with a diameter of about 1 mm was obtained after carbonization. The Si NPs were completely wrapped by the CNFs (Fig. 10b-d). The CNFs could enhance electronic conductivity of the electrode through the formation of continuous electronic pathways and alleviate the large volume expansion of Si NPs. Moreover, the CNFs reduced the surface contact of Si NPs with the electrolyte and prevented the pulverization of Si NPs during cycling. Thus, the resulted Si NPs/CNFs composite exhibited excellent cycling and rate performance. When cycled at a rate of 3 C, only 1% of the initial capacity was lost after 300 cycles (Fig. 10e). Further, increasing the rate from C/10 to 12 C, 52.2% of the original capacity (~750 mAh/g) was still maintained, demonstrating high rate capability and good cycle stability (Fig. 10f).

Recently, a novel Si@HC/CNFs composite with hollow core-shell structured silicon@carbon (Si@HC) NPs embedded in CNFs was prepared via a sol-gel and electrospinning method assisted by an acid treatment step [60], as displayed in Fig. 11. Fig. 11(b-d) showed that the Si@HC particles had a typical core-shell structure and were embedded and dispersed along the CNFs. In accordance with a large number of studies in Section 2.2, the voids between the Si NPs core and carbon shell helped to accommodate the volume expansion of Si associated with the lithiation/delithiation process and allowed formation of a stable SEI film. Besides, superior electrical conductivity was obtained because the CNFs and the carbon shell was good conductor for both electrons and ions. The obtained electrodes exhibited good cycle performance with a high reversible capacity of 1020.7 mAh/g after 100 cycles at a current density of 0.2 A/g (Fig. 11e), and also delivered excellent cycling performance at a high current density of 3.2 A/g (Fig. 11f).

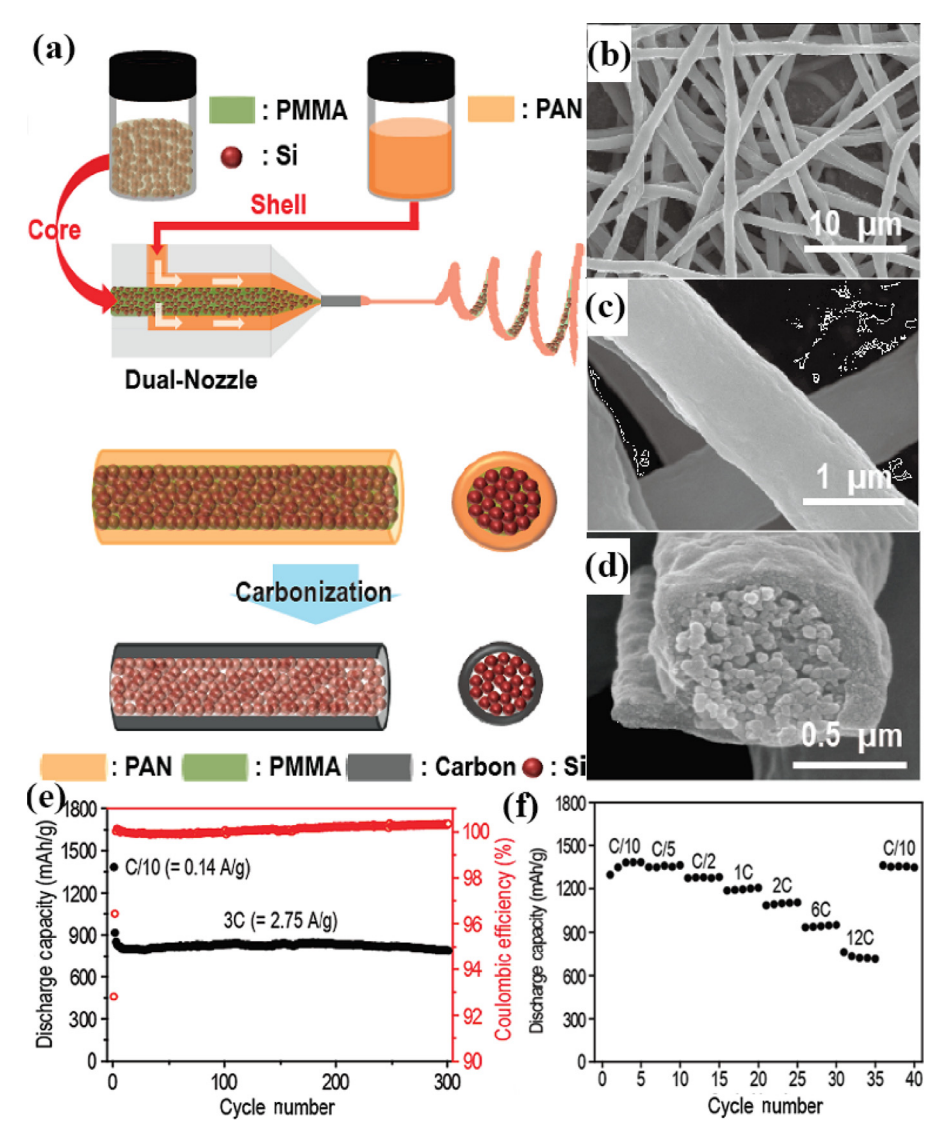


Fig. 10. (a) Si NPs/CNFs nanofibers produced by a dual nozzle electrospinning machine; (b and c) SEM and (d) SEM cross section of 1D nanofiber; (e) Cycling performance of the Si NPs/CNFs composite measured at a 3 C rate and (f) rate capability test for the Si NPs/CNFs composite. Reprinted with permission from Ref. [59]. Copyright (2011) American Chemical Society.

Silicon nanotubes (SiNTs) and silicon nanowires (SiNWs), which possess the same one-dimensional (1D) structure similar to CNTs and CNFs, have the advantage of allowing the expansion of Si in wire diameter without cracks or breaks owing to their facile strain relaxation. Furthermore, once an electrically conductive coating is present on the surface, these 1D SiNWs and SiNTs can possess robust electrical transport along the wire and tube axis, while the Li⁺ transportation can be accomplished radially within a very short distance. Thus, it is well recognized that these 1D SiNWs/C and SiNTs/C composites possess a high specific capacity and superior rate capability with long cycle life. Wang et al. [61] synthesized Si/C nanowires where the Si dwelled in the one dimensional hollow graphitic tubes (GT). Such 1D Si/1D carbon hybrid structure (Si NW-D-GT) constructed a kind of robust line-to-line contact between Si and C, which created efficient channels for fast transport of both electrons and Li+. The Si NW-D-GT composite exhibited good rate capability and remarkable cycling stability (a capacity of 1100 mAh/g at 4200 mA/g over 1000 cycles). That was mainly contributed to the combined characteristic with the built-in void space and the line-to-line contact mode. Jung and co-workers [62] fabricated carbon coated Si NTs using a facile surface sol-gel reaction on easily obtained electrospun organic nanowires, followed by a simple magnesiothermic reduction. The Si NTs showed excellent electrochemical performances (a capacity of about 1900 mAh/g at 400 mA/g with a coulombic efficiency of nearly 100% during cycling) owing to the hollowness of the nanotubes, which allowed them to accommodate the huge volume change during cycling,. Lu et al. [63] used a facile approach to decorate Si NPs with carbon (C@SiNTs) through a CVD process. The as-synthesized C@SiNTs anode delivered a capacity of 2085 mAh/g at 840 mA/g (0.2 C), and a capacity retention of 95% after 200 cycles relative to the capacity value of the 10th cycle. Besides, a high specific capacity (421 mAh/g) could still be achieved, even the current density increased to 20 C. Such high excellent cyclability, and rate performance were originated from the hollow structure of SiNTs and the decorated carbon NPs, which effectively accommodated the strain and improved the electrical conductivity of the whole electrode. Liu et al. [64] presented a carbon-silicon-carbon (C@Si@C) nanotube with sandwich structure to address the mechanical and chemical stability issues of Si. Compared with pure SiNTs, the C@Si@C nanotube array exhibited much better capacity and structure stability. Here, the obtained C@Si@C composite possessed a capacity of ~2200 mAh/g (750 mAh/cm³) and a nearly constant coulombic efficiency of 98% over 60 cycles.

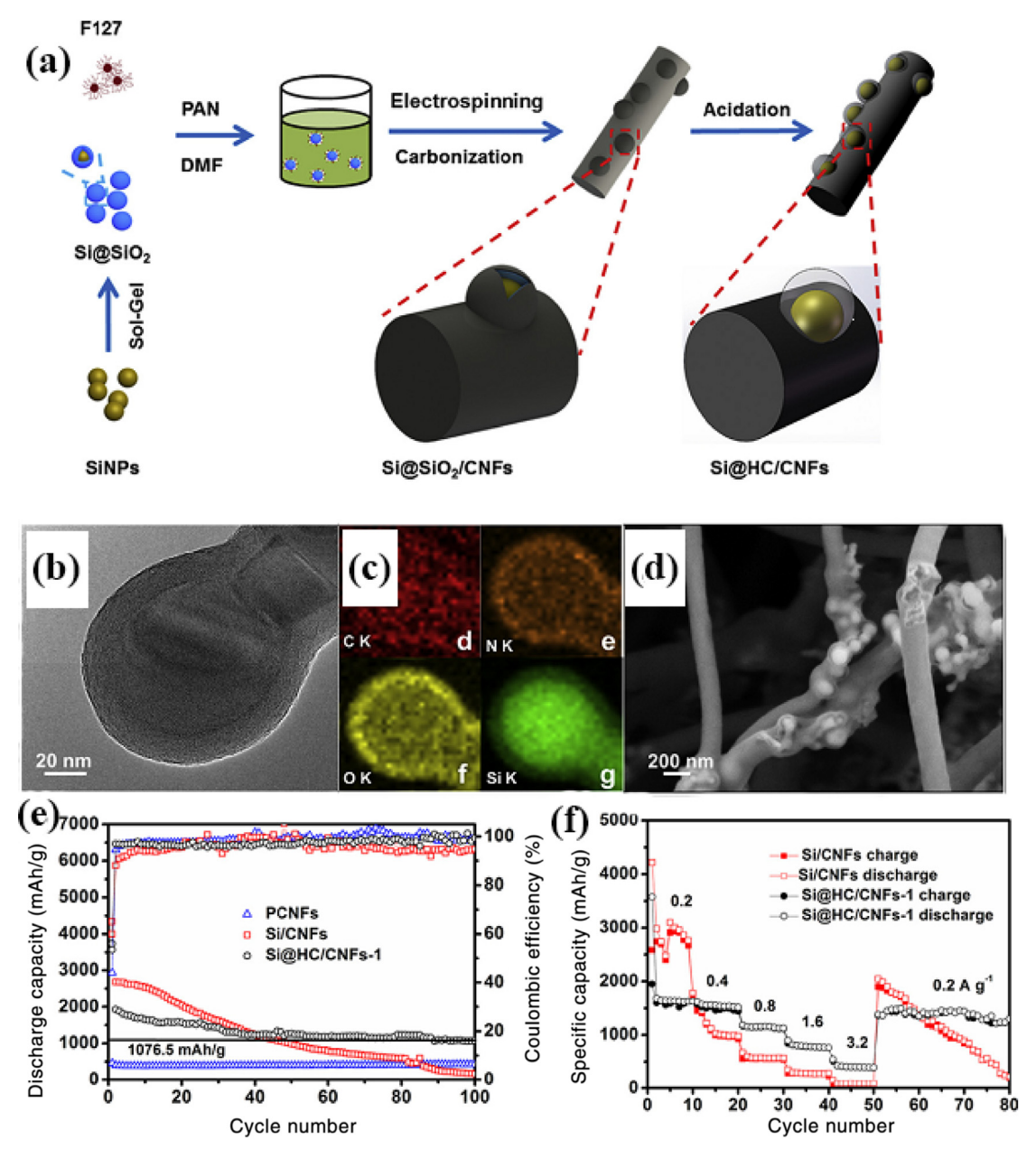


Fig. 11. (a) Schematic of the Si@HC/CNF composite preparation process; (b) TEM image and (c) elemental mapping images of the Si@SiO₂ NPs obtained from the sol–gel method; (d) SEM image of Si@HC/CNFs obtained after selective removal of the SiO₂ sacrificial layer by treatment with HF; (e) Cycle performance, coulombic efficiency at 0.2 A/g and (f) rate capabilities at various rates for the Si/CNF and Si@HC/CNF electrodes. Reprinted with permission from Ref. [60]. Copyright (2017) Elsevier B.V. All rights reserved.

In general, 1D Si/C composites with controlled one-dimensional morphologies, such as SiNWs, SiNTs and Si/CNFs, can effectively facilitate electron transportation and Li⁺ diffusion, improve the rate capability and enhance the cycling stability of the electrode. However, one of the drawbacks for these 1D Si/C composites is their electrode synthesis processes, which is different from that of the current graphite-based electrode adopted commercially. Thus, new electrode making methods at low cost are needed to be developed for these emerging materials. Moreover, increasing mass loadings and decreasing costs are another two main challenges of these 1D Si/C anodes for industrialization manufacture [65].

2.5.3. Graphene

Besides graphite and CNTs/CNFs, graphene is another admirable candidate to composite with Si owing to its outstanding electrical conductivity, large surface area (theoretical value of 2630 m²/g)

and superior mechanical properties (forty times stronger than diamond) [66]. Chou et al. [67] firstly prepared Si/graphene composites by simple mixing in a manual way in 2010. The resulting materials maintained a capacity of 1168 mAh/g and an average coulombic efficiency of 93% up to 30 cycles at 100 mA/g. Lee et al. [68] fabricated Si/graphene composites by simple membrane filtering of a homogeneous mixture of Si NPs and GO in aqueous solution, followed by thermal reduction treatment under an H₂/Ar atmosphere. The Si/rGO composite achieved a capacity of 2200 mAh/g at 100 mA/g after 50 cycles and still maintained about 1500 mAh/g after 200 cycles with a capacity retention of 99.5% per cycle. Ko et al. [69] prepared an amorphous Si NPs backboned graphene nanocomposite (SGC) by pyrolytic decomposition of SiH₄ on reduced graphene, followed by thermal reduction of freeze-dried porous graphene oxide. The SGC exhibited high power capability and excellent cycling stability (a reversible capacity of 517 mAh/g with high initial CE of 92% at 0.5 C, where 96% of

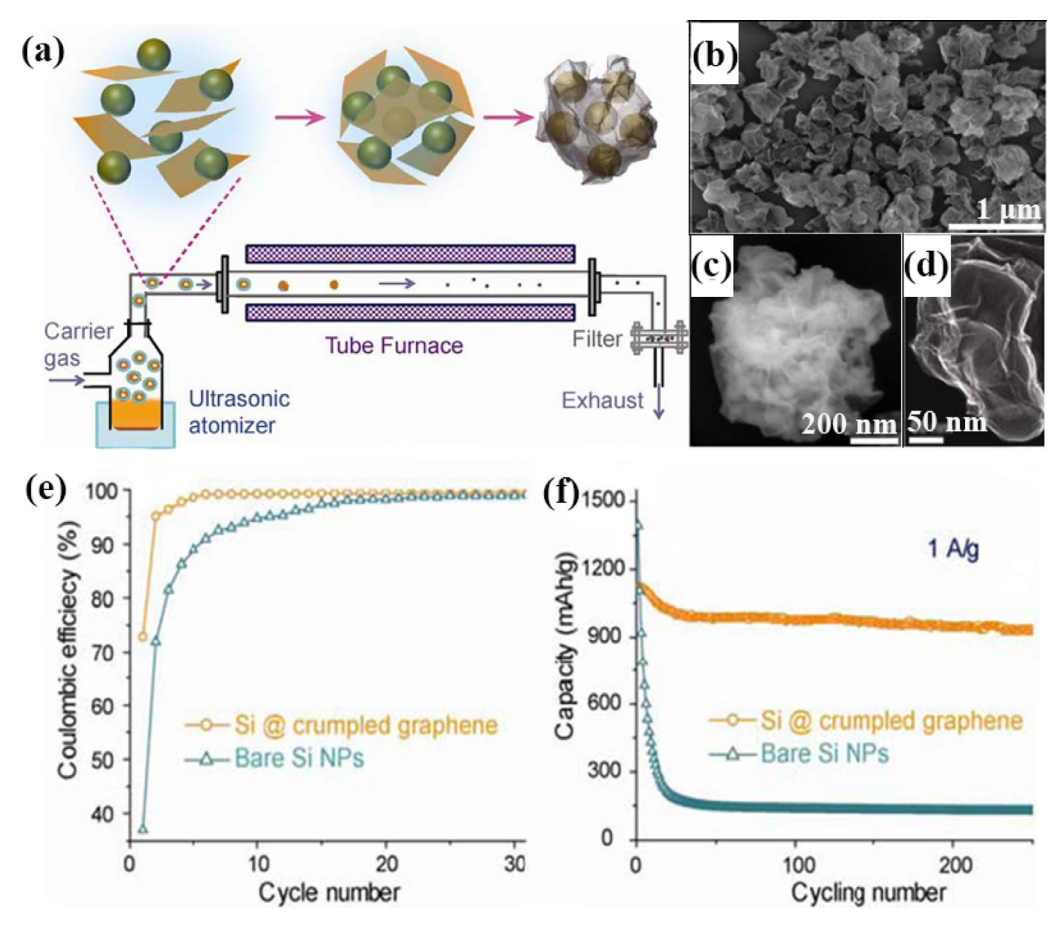


Fig. 12. (a) Schematic illustration of fabricating crumpled-graphene-wrapped Si NPs through an aerosol-assisted capillary assembly method; (b–d) SEM and TEM images of the composites; (e and f) Cycling performance of the composite capsules in comparison with the unwrapped Si NPs at a constant current density of 1 A/g. Reprinted with permission from Ref. [72]. Copyright (2012) American Chemical Society.

capacity was retained after 100 cycles). They combined SGC with $LiCoO_2$ cathode to form LIB full cell with high reversible capacity in the first cycle (162 mAh/g in the voltage range of 2.5–4.3 V) and good rate capability (82% of its initial capacity after 100 cycles at 7C), and a higher energy density (1043 Wh/L) was also obtained compared to the full cell based on routine graphite anode.

Particularly, graphene essentially is a single atom thick layer of sp^2 hybridized carbon in the two dimensional (2D) form with a honeycomb lattice, thus a special kind of Si/graphene composites including encapsulation and sandwich structures can be constructed. The graphene sheets can not only prevent the aggregation and direct exposure to the electrolyte of Si particles, but also serve as skeleton support to buffer the mechanical stress and enhance lithium ion transportation and electrochemical reaction [70]. In an attempt to achieve good cycling performance with a significantly higher volumetric energy density, Son et al. [71] applied multilayer graphene directly grown on the Si NPs surface as a coating material (Gr-Si NPs) by CVD method. Here, such 2D layered character of graphene provided a unique and efficient operation of Si anodes since multilayered graphene shell could accommodate Si volume expansion via a sliding process between adjacent layers. Thus, when paired Gr-Si NPs anode with LiCoO2 cathode to form LIB full cell, high volumetric energy densities of 972 (242.0 Wh/kg) and 700 Wh/L (169.6 Wh/kg) at first and 200th cycle were obtained after 200 cycles at 0.5 C respectively, which were about 1.8 and 1.5 times higher than those of current commercial lithium-ion batteries (550 Wh/L).

Luo et al. [72] devised an aerosol-assisted capillary assembly method to prepare crumpled-graphene-wrapped SiNPs composite, as illustrated in Fig. 12(a). In the process, the colloidal mixture of Si NPs and GO was nebulized to form aerosol droplets, which were blown through a preheated tube furnace at 600 °C with N $_2$ carrier gas. As seen in Fig. 12(b–d), 50–100 nm diameter Si NPs were wrapped in the 5–10 nm thick crumpled graphene shell. The folds and wrinkles in the crumpled graphene capsule could accommodate the volume expansion of Si upon lithiation without losing the integrity of electrode. Compared to bare Si NPs, the Si@crumpled graphene displayed enhanced performance as lithium battery anodes in terms of its cycling stability and coulombic efficiency. The composite delivered a capacity of 940 mAh/g after 250 cycles at a current of 1 A/g with only 0.05% capacity loss per cycle (Fig. 12e and f).

Zhou et al. [73] prepared Si/graphene composite via a selfassembly method (Fig. 13a), which was an effective strategy for forming ideally mixed nanocomposites. Due to the inherent surface oxide layer on Si NPs and the ionization of the carboxylic and phenolic hydroxyl groups on GO, both Si NPs and GO had negative charges in aqueous solution. Thus, Si and GO could be self-assembled together in the presence of poly(diallyldimethylammonium chloride) (PDDA), which served as a positively charged medium to attract GO and Si. The self-assembly suspension was thermally reduced to yield welldispersed Si NPs encapsulated in graphene (Si-NP@rGO). The Si NPs were well wrapped by graphene sheets of about two layers to form a bulge-like micrometer-sized structure (Fig. 13b-e). When cycling in the voltage range of 0.05-1.0 V at 100 mA/g, the Si-NP@rGO displayed quite stable cycling performance and delivered a capacity of 1205 mAh/g after 150 cycles (Fig. 13f). As the

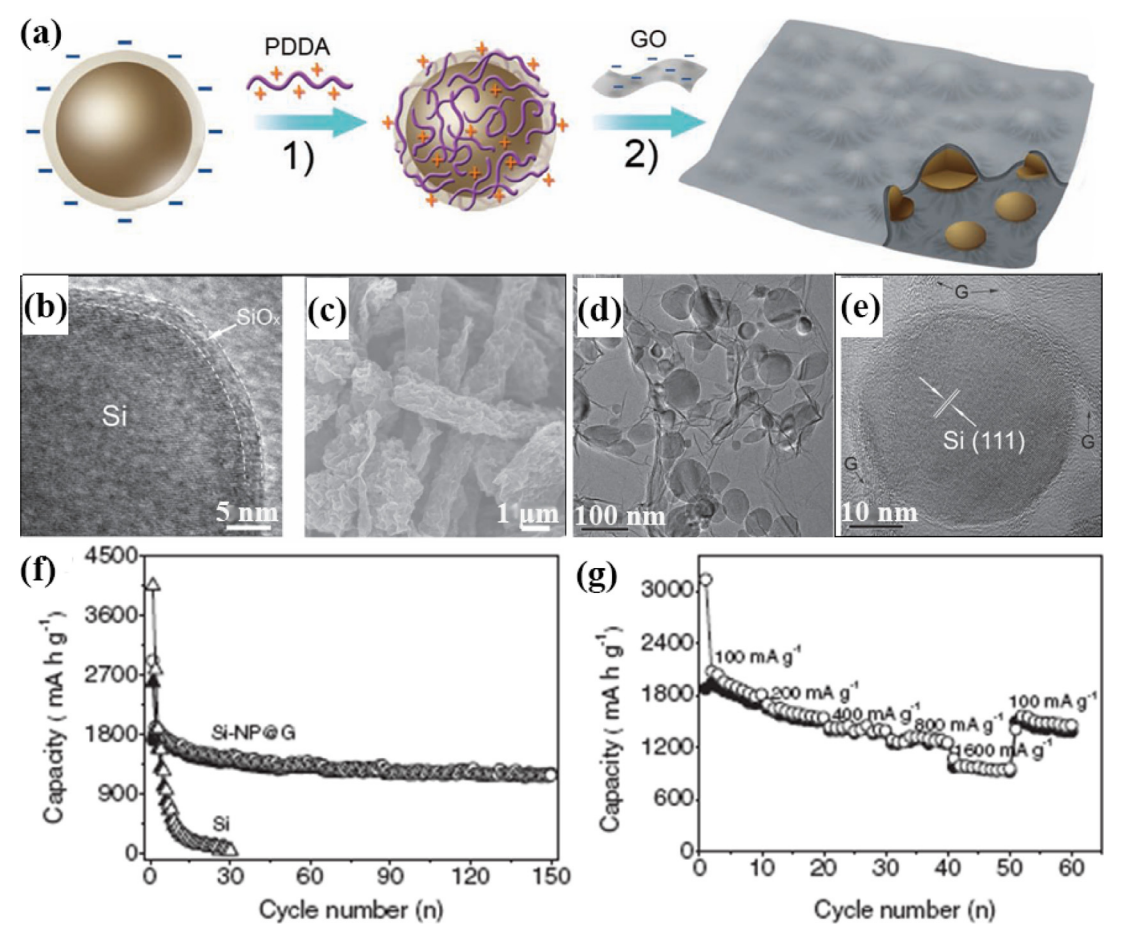


Fig. 13. (a) Fabrication process of the Si-NP@G composite; (b-e) SEM and TEM images of the SiNP@G nanocomposite; (f) Cycling test and (g) rate performance of the Si-NP@G composite. Reproduced with permission from Ref. [73]. Copyright (2012) WILEY-VCH Verlag GmbH & Co. KGaA, Weinheim.

current density increased from 100 to 1600 mA/g, the Si-NP@rGO composite still possessed a reversible and stable capacity of 990 mAh/g (Fig. 13g).

Recent researches find that such unique sandwiched structure plays a vital role in enhancing the performance of Si/graphene composites [74]. In this configuration, the alternately stacked elastic layers of graphene sheets construct hierarchically porous structures which could offer adequate void space to accommodate Si materials, and the inside void space can mitigate the volume expansion of Si and buffer the strain during the lithium intercalation/de-intercalation process. Mori et al. [75] fabricated Si/graphene multilayer sandwich structures by an electron beam deposition method without air exposure. It was found that different numbers of layers and thickness of each layer for this sandwich structure directly influenced the properties of first discharge capacity, coulombic efficiencies, and reversible efficiencies of batteries. The results showed that the structure with seven layers which are 100 nm thick, possessed the best discharge capacity over 1600 mAh/g at a current density of 100 mA/g after 30 cycles. Liu et al. [76] designed rolled-up Si/reduced graphene oxide bilayer nanomembranes with sandwich architecture. It was found that the inner void inside the configuration together with the mechanical feature of the nanomembranes severed as an effective buffer medium to prevent the Si from inflating and crushing during lithiation/delithiation. Furthermore, the alternately aligned rGO layers could not only enhance electronic conductivity, effectively release the volume change and aggregation of Si NPs, but also could protect the nanomembranes from excessive formation of thick SEI layers during the charge/discharge process. As anodes for LIBs, this

sandwiched Si/rGO nanomembranes possessed a long cycling life of 2000 cycles at 3 A/g with a capacity degradation of only 3.3% per 100 cycles.

Besides, the unique conductive function of graphene plays an important role in linking all Si particles together regardless of their distance from the current collector, which provide an approach to high areal capacities with high mass loading. Zhou et al. [77] fabricated Si NPs/graphene composite film by electrostatic self-assembly of bovine serum albumin (BSA)-decorated Si NPs and GO sheets during vacuum filtration followed by thermal annealing, in which the oriented graphene sheets were bridged by the Si NP-templated carbon hinges. Such assembled configuration accommodated the volume change of the impregnated Si NPs and facilitated the transport of electrons and Li ions, thus the electrode with a high packing density of $\sim 1.3 \, \text{g/cm}^3$ exhibited a gravimetric capacity of ~1390 mAh/g after 200 cycles at 2 A/g with a capacity fade of only 5%. The volumetric capacity (1807 mAh/cm³) was almost four times than that of the commercial graphite anodes (440-600 mAh/cm³), while the electrode with high mass loading of 3.7 mg/cm² displayed an areal capacity of 6.0 mAh/cm² (1622 mAh/g) after 100 cycles at 3.0 mA/cm² (0.8 A/g).

The studies in this area reveal that the addition of graphene can improve capacities and cycle stability of Si anodes to a certain degree, but graphene compositing with Si alone does not guarantee good electrochemical performance completely. Because it is difficult for the graphene to realize entire silicon capsulation, even if it has high electronic conductivity and good flexibility. Here, the best electrochemical performance is obtained from the synergistic

functions of graphene, amorphous carbon and Si nano-particles [4]. Zhou et al. [78] carried out further research on multiple composites of anode in order to achieve a better electrochemical performance for LIBs. A double protection strategy was employed to fabricate Si/graphene/amorphous coating carbon hybrid anodes so as to further improve the electrical conductivity and structural stability. The graphene and the amorphous carbon coating layers worked together to effectively accommodate the volume expansion, and suppress the aggregation and destruction of the Si particles. As a result, a discharge capacity of 902 mAh/g was maintained after 100 cycles at a current density of 300 mA/g. The synergistic effects of graphene, amorphous carbon coating and Si particles were further researched by Yi et al. [79]. The procedure started with mixing micro-sized SiO and GO in water in the presence of poly(diallyldimethylammonium chloride) (PDDA) which served as a positively charged medium to attract SiO and GO. Subsequently, the GO/PDDA-SiO mixture was heated to 950 °C for 5 h, followed by HF etching at room temperature to create micro-sized porous Si supported by graphene. Finally, carbon coating was deposited onto the surface of Si/graphene by thermal decomposition of acetylene. The porous Si/graphene/amorphous coating carbon (rGO/Si-C) composite exhibited a high specific capacity (~1150 mAh/g) and remained at this level after 100 cycles due to the synergistic effects of the carbon coating, graphene support and porous Si with nano-sized building blocks. The introduction of graphene provided additional electron pathways and constructed conductive networks among Si particles. Such well-engineered structure allowed a higher degree of material utilization at high mass loading compared to raw carbon-coated, micro-sized porous Si composite (Si@C) without graphene. Thus, a high areal capacity of 3.2 mAh/cm² after 100 cycles and high coulombic efficiency (average 99.5% from 2nd to100th cycle) were achieved by rGO/Si-C, whereas the specific capacity of the Si@C decreased sharply by high mass loading. Wu et al. [80] also synthesized a novel binderfree Si/graphene/porous carbon composite film consisting of alternately stacked Si, graphene layers and porous carbon layers by an electrostatic spray deposition and subsequent heat treatment method. It was found that the layer-by-layer porous carbon framework could suppress the volume expansion of Si particles efficiently, while the flexible graphene layer was capable of facilitating electron transport and maintaining structural integrity of the electrode. This hierarchical architecture displayed a reversible capacity of 1020 mAh/g at 200 mA/g with 75% capacity retention after 100 cycles.

Recently, Agyeman et al. [81] prepared a novel silicon/carbon/graphene (Si@C-rGO) composite with sandwich structure assembled by commercial Si NPs, dopamine hydrochloride and GO solutions via a simple stirring and vacuum filtration method, the schematic illustration of the fabrication process was shown in Fig. 14(a). In this configuration, Si@C nanoparticles were firmly held and anchored within the sandwich structure of the wrinkled graphene sheets via strong covalent and hydrogen bonding from polydopamine linkers (Fig. 14b and c). Herein, a high gravimetric capacity (1001 mAh/g at 300 mA/g) and a long cycle life (93% over 400 cycles) were simultaneously achieved with the Si@C-rGO composite (Fig. 14d). Moreover, excellent rate performance was obtained (a high capacity of 767 mAh/g at a current density of 3 A/g), proving the excellent kinetic property of the Si@C-rGO composite (Fig. 14e). Excellent volume suppression was also recorded with less than 10% volume change. Such excellent electrochemical performance was ascribed to the synergistic functions of the uniform distribution of Si NPs, carbon coating, and graphene sheet supported sandwich structure, which effectively prevented aggregation and pulverization of Si NPs, kept the overall electrode highly conductive, and maintained the stability of the structure.

3. Other factors affecting the performance

Si/C composite with excellent capacity and appropriate cycle life is a promising alternative anode material. However, most of these phases suffer from inferior initial CE. This drawback primarily originates from Li⁺ trapping in the matrix and the formation of unstable SEI layer in the first cycle, which is clearly related to the degree of Si expansion during lithiation. Such high irreversible capacity from the anode will decrease the energy density of the full Li-ion batteries. Here, multidisciplinary studies of prelithiated, electrolyte additives and polymeric binders are discussed about how to enhance the electrochemical performance of Si-based anodes, especially the initial CE.

3.1. Prelithiated

Prelithiation treatment has been considered to be one of the most proper methods to conquer the inferior initial CE of Si-based anodes for real applications of LIBs. Prelithiation methods can be divided into two aspects: electrochemical plating and chemical reaction method. The concept of electrochemical plating is quite straightforward: to cycle the anode with lithium metal or other counter electrode with the aid of electrolyte before assembling it into a practical Li-ion battery. Zhou and Wang [82] designed an electrolytic cell to form a prelithiated Si electrode by combining a Cu pitting corrosion type anodic half-cell in Li₂SO₄ aqueous electrolyte with a Si lithiation type cathodic half-cell in gel polymer electrolyte which was soaked in LiPF₆/EC + DEC. The two half cells were separated by a lithium super ionic conductor film (Li₂O-Al₂O₃-SiO₂-P₂O₅-TiO₂-GeO₂) and the Cu wires were used as the counter electrode. The final prelithiated Si/C electrode was produced by a subsequent floating-catalyst method, carbon covering and in situ generating carbon-nanotube framework. The authors assembled MnO_x/Si full cells using the prelithiated Si anodes, achieving a high specific energy of 349 Wh/kg at a specific power of 20 W/kg. The full cell still retained 138 Wh/kg even at a high specific power of 1710 W/kg. Although the improvement in electrochemical performance was significant, the realizing of this method was complex and not very valuable to practical application, thus resulting in being mostly employed in laboratory.

With respect to chemical reaction method, lithiation is obviously achieved by utilizing chemical reaction between the active material and other chemical reagent. Lithium metal powder is the mostly used lithiation reagent. To apply lithium metal powder into the anode electrodes, two different methods have been applied: lithium metal powder is either added into electrode slurry for film casting, or loaded directly on top of dried anode laminate. Currently, the only commercial prelithiation reagent in powder form is microscale stabilized lithium metal powder (SLMP) with a mean diameter of 10-50 μm developed by FMC Lithium Corp. Unlike the normal Li powder, SLMP can be handled safely in dry air, due to the covered passivation layer (Li₂CO₃, 100-1000 nm) on the surface of SLMP. Besides the above advantage, the Li loading amount can be controlled and adjusted easily while the Li powder can be distributed uniformly throughout the electrode. SLMP reacts upon adding electrolyte to the cell and forms a SEI layer which can compensate the irreversible capacity during the first cycle and thus enhance the energy density significantly. Forney et al. [83] used pressure-activated SLMP to prelithiate silicon/carbon nanotubes (Si/CNT). The introduced lithium compensated for its consumption during the SEI formation process, hence resulting in increased reversible capacity particularly in the first cycle. The prelithiated treatment on Si/CNT anode eliminated 20-40% of irreversible capacity loss in the first cycle. When it was coupled with lithium nickel cobalt aluminum oxide (NCA) cathode, the full cell

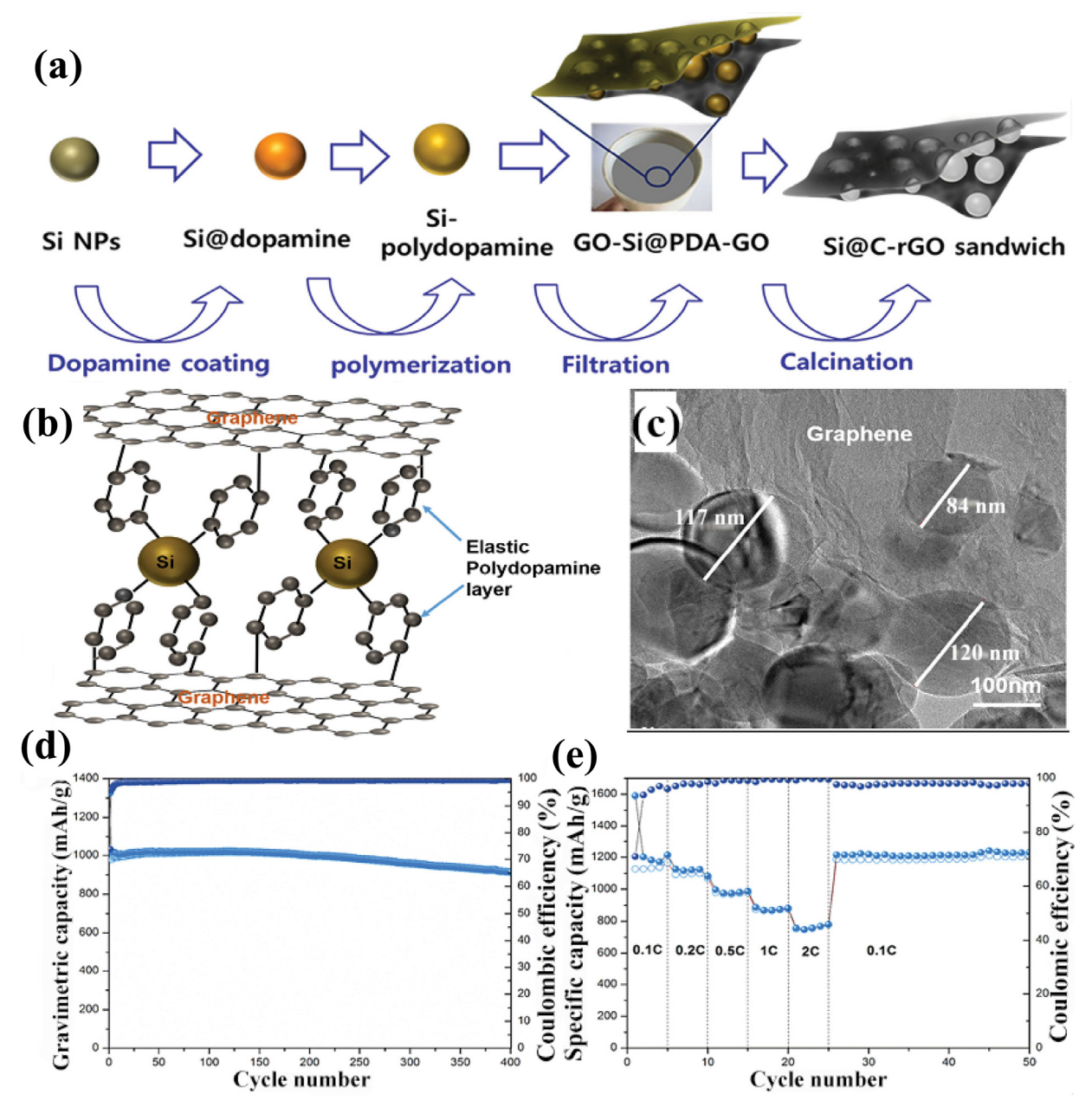


Fig. 14. (a) Schematic illustration of the fabrication processes of the sandwich-structured Si@C-rGO composite and (b) the strongly anchored Si NPs to graphene sheets via strong covalent and hydrogen bonding from polydopamine linkers; (c) TEM image of Si@C-rGO composite; (d) Cycling performance of Si@C-rGO over 400 cycles; (e) Charge/discharge capacities at various rates. Reproduced with permission from Ref. [81]. Copyright (2016) WILEY-VCH Verlag GmbH & Co. KGaA, Weinheim.

retained 93% of the initial capacity at 100% DOD and even obtained >1000 cycles at 20% DOD. Yao et al. [84] fabricated novel freestanding flexible Si nanoparticles-multiwalled carbon nanotubes (SiNPs-MWNTs) composite paper anodes through a combination of ultrasonication and pressure filtration. The SLMP prelithiation approach was employed to improve the first coulombic efficiency. Further, they examined the effect of SLMP loading on the battery chemistry, and found that an SLMP/anode mass ratio of 0.26 led to the optimal initial reversible capacity. The first discharge and charge capacities of the regular half-cell without SLMP displayed 2298 and 1492 mAh/g with a coulombic efficiency of 65%, respectively. While the SLMP cell yielded a capacity loss of 28 mAh/g and a raised first coulombic efficiency of 98%. The voltage profile revealed that the absence of the plateau at ~0.7-0.8 V representing the decomposition of electrolyte and the formation of SEI layer on anode surface during the first discharge of the SLMP cell, which also suggested that the SEI formation process disappeared during its first discharge.

Pan et al. [85] coated SLMP on the surface of D-SiO/G/C anode, the initial coulombic efficiency was improved from 68.1% to 98.5%. Moreover, the SLMP prelithiated micro-sized D-SiO/G/C composite retained an excellent cycling retention of 95% after 200 cycles (Fig. 15). Although this method seems easy for industrialization and SLMP is stable in dry air, SLMP is prone to dust, leading to environmental pollution and potential safety risk. What's more, SLMP is very expensive which only can be supplied by FMC corporation and hence brings about high manufacturing cost. Therefore, there are still many challenges for proper utilizing of lithium powders in large scale.

Kim et al. [86] proposed a novel prelithiation method to pretreat $c\text{-SiO}_x$ based on electrical shorting with lithium metal foil in the presence of an optimized circuit resistance. The accurate short-

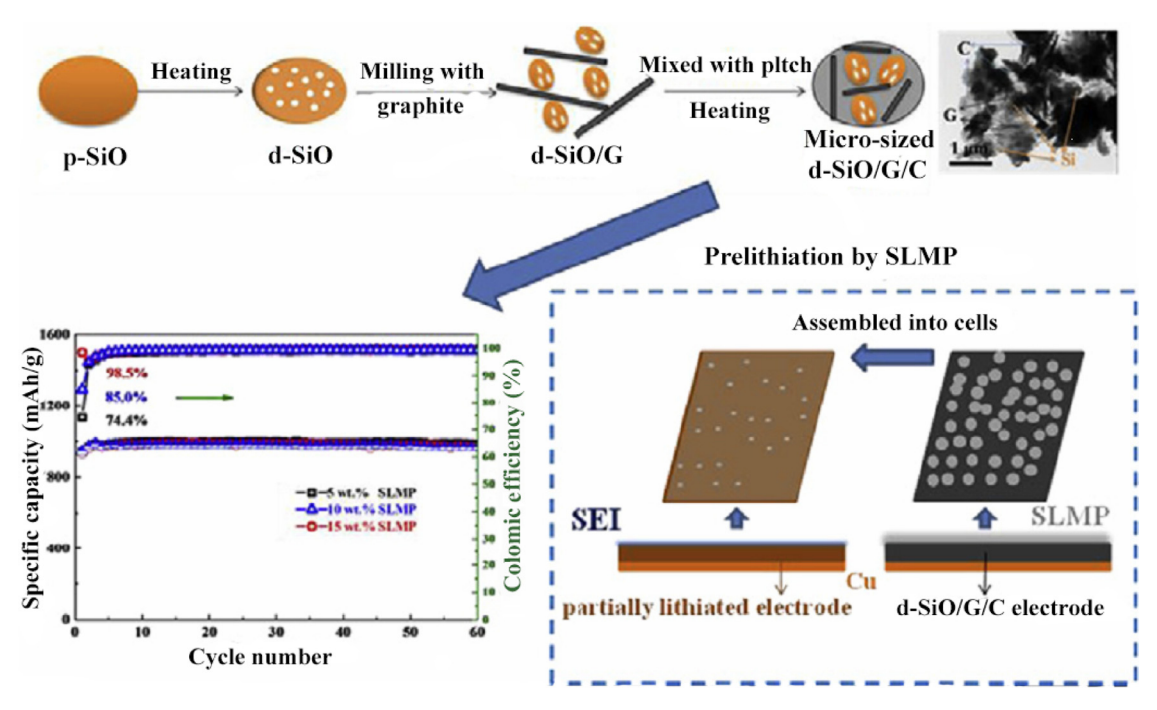


Fig. 15. The preparation process of micro-sized D-SiO/G/C composite and cycle performances and coulombic efficiencies of D-SiO/G/C prelithiated by SLMP (10 wt%). Reprinted with permission from Ref. [85]. Copyright (2017) Elsevier B.V. All rights reserved.

ing time and voltage monitoring allow a fine-tuning on the degree of prelithiation. This technique allows the initial coulombic efficiency as high as 94.9% without sacrificing the structural stability of SiO_x at all throughout cycling. Full-cells upon integration with LiNi_{0.8}Co_{0.15}Al_{0.05}O₂ (NCA) exhibited enhanced first discharge capacity of 165.1 mAh/g_{NCA} and a commercial level of initial areal capacity (2.4 mAh/cm²). Cao et al. [87] developed a trilayer structure of active material/polymer/lithium anode to realize the prelithiation of the Si-based anode. In these electrodes, metallic lithium was first protected by a PMMA layer against air and moisture, then Si-based active materials were coated onto PMMA. PMMA was readily soluble upon contacting with battery electrolytes, and active materials were in situ lithiated to form a lithiated anode. With this strategy, they acquired excellent initial coulombic efficiency of over 100% in Si NPs anodes owing to the prelithiation "charges" prior to electrochemical lithiation. Thus, there was only little capacity loss in the initial charging due to SEI formation. The lithiated anodes revealed higher cycling stability of 1456 mAh/g after 100 cycles than bare silicon (809 mAh/g after 100 cycles).

Although these novel strategies realize remarkable enhanced performance (especially initial CE) of Si-based anodes, they may not be practical in industrialization. The chemical lithiation of anode is more difficult than cathode material, a more reactive lithium source is needed and the lithiation product is usually unstable and hard to control. The prelithiation of silicon anode is seriously insufficient to tackle these problems up to now. Nevertheless, several suitable prelithiation methods and capacity compensation solution is developed, the practical application of silicon-based anode will become more attractive for achieving high energy density.

3.2. Electrolyte additives

As for Si-based electrodes, the SEI generated on the Si surface is usually unstable, leading to the growth of a thick SEI and ultimately poor initial capacity and low first CE. Thus, building a robust SEI layer on the Si is pivotal to improve the performance of Si-based anode. Electrolyte additive, capable of passivating the Si/electrolyte interphase and forming a stable SEI, is a promis-

ing strategy to integrate structural integrity with stable interfacial chemistry. A variety of electrolytes additives including vinylene carbonate (VC) [88,89], tris(pentafluorophenyl)borane [90], succinic anhydride [91,92], and fluoroethylene carbonate (FEC) have been investigated in the last decade for silicon anode. Among them, VC and FEC are identified as effective additives for enhancing the CE and capacity retention of Si anode.

Chen et al. [89] reported that in the presence of 1 wt% VC in EC:DMC (1:1 in volume) containing 1 M LiPF₆, both coulombic efficiency and cycling stability of the Si electrode were improved. The initial CE was increased from 67.9% to 72.5%, while the reversible capacity in VC-containing electrolyte was stable at ~2000 mAh/g even up to 200 cycles, and gradually decayed to more than 500 mAh/g after 500 cycles. The improvement in the electrochemical performance of Si anodes by the FEC additive was attributed to the advanced properties of SEI layer with smooth and uniform morphology formed in initial several cycles. Choi et al. [93] found that the coulombic efficiency of the Si anode was increased by over 99% after 80 cycles with the introduction of FEC, while the coulombic efficiency without the addition of FEC dropped to ~97% after 80 cycles. That was mainly attributed to the smoother and stable SEI layer structure by the introduction of FEC into the electrolyte. The research conducted by Nakai et al. displayed that the addition of FEC into the electrolyte (50% v/v%) could increase the discharge capacity of Si anode from approximately 2750 mAh/g to above 3200 mAh/g. Besides, the coulombic efficiency of the electrode was also enhanced from about 98% to more than 99.5% after 30 cycles.

Xu et al. [94] also utilized an FEC-containing electrolyte (FEC, 10 wt%) for Si NPs based anode with only 5% capacity (referring to 1200 mAh/g) was lost and coulombic efficiency of about 99% was retained after 80 cycles. Whereas, only 70% capacity of the electrode in the FEC-free electrolyte was preserved and the coulombic efficiency dropped to ~97% after 80 cycles (Fig. 16). Such superior electrochemical performance of Si anodes in FEC-containing electrolyte was well investigated and attributed to the formation of stable SEI film derived from FEC [94,95]. Etacheri et al. [96] believed that FEC first converted into vinylene carbon-



Fig. 16. Possible FEC decomposition reactions and schematic representation of SEI formation on a silicon anode cycling with FEC/LP40. Reprinted with permission from Ref. [94]. Copyright © 2015, American Chemical Society.

ate through defluorination and vinylene carbonate then polymerized to form a polycarbonate species. Recently, it was found that the reduction products of FEC mainly consist of -CHF-OCO₂ type compounds and LiF. The resulted compounds formed an initial SEI which covered the Si surface evenly. Such initially formed SEI film was mechanically strong enough to prevent the formation of large amounts of cracks, so as to alleviate the constant decomposition of the electrolyte and thus prevented the continuous generation of a non-uniform SEI layer. In addition, another product LiF was favorable for the conductivity of Li⁺ in the SEI film.

3.3. Binders

In addition to active material and electrolyte, the properties of binders also play a critical role in cycle stability and initial CE of Sibased electrode. Poly(vinylidene fluoride) (PVDF) is commercially used as a binder in graphite anode batteries with good cementation properties. Unfortunately, this binder cannot accommodate the large volume variation of Si-based anodes between fully lithiated and delithiated states because of its weak van der Waals interactions. Recently, considerable progress has been made in the utilization of new functional binders, which have stronger adhesive properties than conventional PVDF binder, to maintain the integrity of Si electrodes and thereby to achieve repeatable LIBs operation. For example, polymer binders containing carboxyl functional groups and their derivatives, such as carboxymethyl cellulose (CMC) [97], polyacrylic acid (PAA) [98] based polymers and alginate (Alg) [99–101] based polymers are employed as binders

for Si anodes. These polymer binders possess much strong interacting ability with Si in comparison to PVDF, which originate from the formation of hydrogen bonding and/or covalent chemical bonds between them. Kovalenko et al. [101] found that Algbased Si anode displayed better electrochemical performance (a reversible capacity over 1700 mAh/g after 100 cycles at a current density of 4.2 A/g) than that of CMC-based Si (below 1.0 Ah/g) under the same conditions. That mainly resulted from the naturally present and evenly distributed carboxyl groups in the Alg polymer chain, whereas in CMC the distribution was random. In addition, multi-functional polymer based on these binders mentioned above has also been developed [102,103]. Ryou et al. [103] designed a binder polymer by conjugating adhesive catechol functional groups stemming from dopamine hydrochloride to PAA and Alg backbones. Such mussel-inspired binders endowed Si NP electrodes (Si-Alg-C and Si-PAA-C) with improved battery performance compared to their counterparts without catechol groups. Si-Alg-C and Si-Alg electrodes exhibited reversible capacities of 3440 and 3250 mAh/g with same coulombic efficiencies of 60.1%, while Si electrodes with PAA-C (Si-PAA-C) and PAA (Si-PAA) displayed reversible capacities of 3500 and 3180 mAh/g with coulombic efficiencies of 71.2% and 72.3%, respectively. That was primarily attributed to the enhanced adhesion by the catecholic interactions, which allowed a larger proportion of Si NPs to participate in the alloying and de-alloying reactions with Li⁺. Besides, the author also anticipated that the overall trend of capacity retention during cycling was mainly affected by the binder backbone, while the catechol functional groups were contributed to the capacity

Accordingly, the incorporation of such functional groups endow the polymer chain with higher adhesion, which is associated with good performance of Si anode, but the linear chain of these polymer binders is susceptible to sliding upon the continual volume variation of Si during cycling [8]. In order to combat this issue, three-dimensional (3D) polymer networks were sequentially synthesized for the Si anodes, in which the polymer chain was anchored by a cross-linking method [104–107]. Koo et al. [104] presented a 3D interconnected network of poly(acrylic acid) (PAA) and sodium carboxymethyl cellulose (CMC) by a condensation reaction. This binder showing no swelling in commercialized electrolytes would prevent any large movement and effectively maintained the

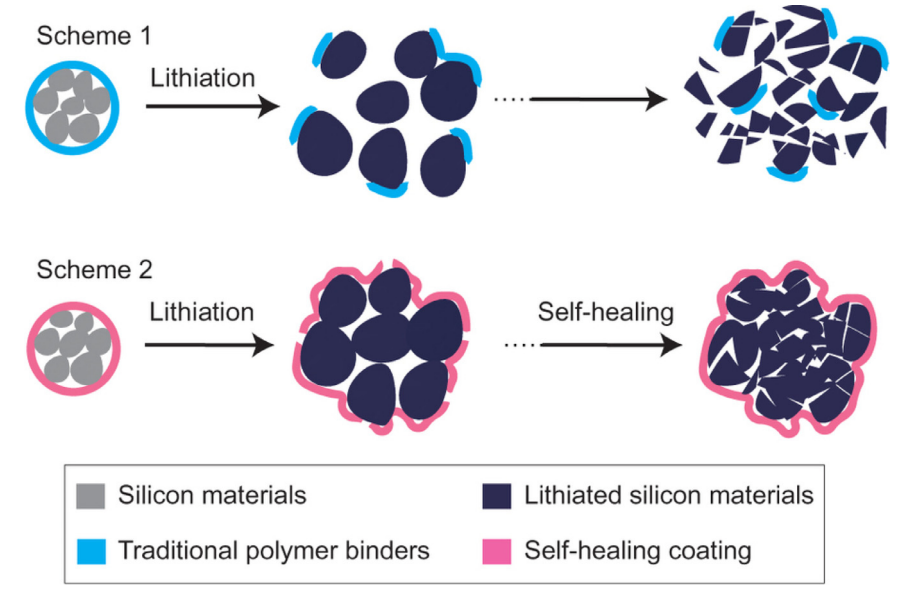


Fig. 17. Schematic illustration of the design of a conventional silicon electrode (Scheme 1) and the stretchable self-healing electrode (Scheme 2). Reprinted with permission from Ref. [109]. Copyright (2013) Rights Managed by Nature Publishing Group.

Table 1. Synthesis strategies and electrochemical performance comparison of Si/C-based anode materials in LIBs.

Anodes	Specific capacity (mAh/g)	Cycling stability (mAh/g)	Rate capability (mAh/g)	Structure	Method	Refs
Si/C	741.2	611.3 after 100 cycles at 0.3 A/g	480.3 at 4 A/g	Si/graphite@N-doped carbon core-shell structure	Spray-drying and carbonization process	[17
Si/p-C(N-SPC)	2262	1607 after 100 cycles at 0.4 A/g	1050 at 10 A/g	Nanostructured silicon/porous carbon spherical	Hydrothermal process and soft template method	[18
Si@SiO ₂ @C	911	785 after 100 cycles at 0.1 A/g	_	Double-walled core-shell structure	Calcination of Si NPs and carbon coating method	[20
Si@SiO _x @C	1980	1450 after 100 cycles at 0.1 A/g	1230 after 100 cycles (500 mA/g)	Double-walled core-shell structure	Ball-milling and carbonization	[10
Si@void@C	813.9	500 after 40 cycles	_	Yolk-shell structure	Template method and carbon deposition	[2
Si@void@meso-C	1272	~1000 after 400 cycles	620 at 8.4 A/g	Yolk-shell structure	Template-based method and a nanocasting strategy	[2:
Si@C@void@C	1910	\sim 1356 after 50 cycles at 0.1 A/g	1146 at 4 A/g	Core-shell and yolk-shell	Template method and carbon deposition	[24
Si@void@SiO ₂ @void@C	~1147	956 after 430 cycles at 0.46 A/g	250 at 5.8 A/g	Dual yolk-shell structure	Template method and carbon deposition	[2
Porous Si/C	1628	759 after 30 cycles at 50 mA/g	776 at 2.0 A/g	Porous structure	Magnesiothermic reduction and carbonization	[3
Porous Si/C	2265	1552 after 200 cycles at 0.2 A/g	1057 at 2.0 A/g	3D interconnected porous Si/C architectures	Magnesiothermic reduction	[3
Mesoporous Si/C	~1500 (0.1 A/g)	990 after 1000 cycles at 1.0 A/g	_	Mesoporous nanostructure	Magnesiothermic reduction and carbon coating by CVD	[3
Porous Si@C nanotube	1276	\sim 1300 after 200 cycles at 0.2 A/g	\sim 580 at 3.2 A/g	Porous coaxial nanotubes	Layer-by-layer assembly on ZnO nanorod templates	[3
Porous Si/C Mesoporous Si@C	856.5 1375	732.1 after 100 cycles 1054 at 50 mA/g after 100 cycles	437.2 at 1 A/g 628 at 2 A/g	Porous structure Porous cage-like structure	A Rochow reaction Template-based carbonization and magnesiothermic reduction	[3 [4
Si@SiO _x @C	1972	1030 over 500 cycles at 0.5 A/g	1030 at 2 A/g 670 at 4 A/g	Dual core-shell structure	One-step pyrolysis method	[4
Si-SiO _x @C	1561.9 at 0.06 C	~1195 after 100 cycles at 1 C	~1360 at 1 C	Si embedded in SiO _x matrix with carbon layer	Spray pyrolysis and simple washing step	[4
Si/graphite	1702.9	975.7 after 100 cycles at 0.1 A/g	672.2 at 5 A/g	Sheet-like morphology	Magnesiothermic reduction	[4
Si/graphite/PAN-C	660	Stable over 30 cycles at 0.16 A/g	-	Embedding structure	Thermally decomposed method	[5
Si/graphite/carbon	~450	>400 after 300 cycles at 0.5 A/g	200 at 5 A/g	Si@flake-graphite/amorphous- carbon microspheres	Ball-milling and spray drying	[5
Si@C/CNTs&CNFs	2169	1195 after 50 cycles at 0.3 A/g	_	Si@C interweaved with CNTs and CNF	Ball milling, spray drying and CVD methods	[5
Si/CNTs	~2050	\sim 1000 after 100 cycles at \sim C/10	\sim 1000 at \sim 2.5 C	Si droplets deposited directly on VACNTs	A simple two-step CVD method	[5
Si/CNTs	3000 (1.3 C)	800 after 100 cycles at 10 C	1900 at 5 C 760 at 15 C		A two-step CVD process	[5
Si NPs/CNFs	1384 (C/10) ∼900 (3 C)	\sim 890 after 300 cycles at 3 C	721 at 12 C (9.75 A/g),	Si NPs wrapped by CNFs	Electrospinning process using a dual nozzle	[5
Si@HC/CNFs	1995.2	1020.7 after 100 cycles at 0.2 A/g	400 at 3.2 A/g	Hollow Si@HC NPs embedded in CNFs	· ·	[6
SiNTs@C	2085	1980.75 after 200 cycles at 0.2 C	421 at 20 C,	Carbon decorated Si nanotubes		[6
Si/graphene	2200	1500 after 200 cycles at 0.1 A/g	_	Si/graphene composites	Membrane filtering and thermal reduction treatment	[1
Si/graphene	1665	>1600 after 100 cycles at 0.1 A/g	672.2 at 2 A/g	Sheet-like morphology	Magnesiothermic reduction	[7
Si/rGO	2871	1433 after 100 cycles at	571 after 3000 cycles at	Sandwich nanoarchitecture	Strain released strategy	[7
Si/C/graphene	1650	0.1 A/g 760 after 100 cycles at 0.2 A/g	3 A/g 508 at 2 A/g	Multilayer structure	Electrostatic spray deposition and heat	[8
Si@C-rGO	1001	931 over 400 cycles at 0.3 A/g	767 at 3 A/g	Si@C anchored within the sandwich structure of wrinkled graphene	treatment A simple stirring and vacuum filtration method	[8

silicon-binder bond strength. Thus, the Si NPs electrodes with this binder exhibited better cycling stability than CMC, PAA and PVDF. A high reversible capacity of over 2000 mAh/g after 100 cycles at 30 $^{\circ}\text{C}$ was obtained and a superior capacity of 1500 mAh/g at higher current density of 30 A/g at 60 $^{\circ}\text{C}$ was maintained.

Recently, self-healing polymers (SHPs) containing abundant hydrogen bonds are designed as binders to stabilize Si anodes. SHPs are able to heal themselves repeatedly and recover functionalities despite being subjected to fractures and damages during battery cycling [108,109]. Wang et al. [109] have utilized a SHP binder

to improve the cycling stability of low-cost silicon microparticles (SiMPs) anodes. Compared with PVDF, CMC and Alg binders, the SHP binder possessed both mechanical and electrical healing capabilities, which allowed the cracks of the conduction paths healing spontaneously and repeatedly during cycling (Fig. 17). Thus, the first cycle discharge capacity of 2617 mAh/g at 0.4 A/g for the SiMPs-SHPs electrode was achieved while 80% of this value was retained after 90 cycles. This was in contrast to SiMP anodes with PVDF, CMC and Alg, which demonstrated poor stability and retained only 14%, 27% and 47% of their initial capacities after 20 cycles at the same current density (0.4 A/g). More recently, the same researchers have designed a novel Si electrode with 3D spatial distribution of SHP binders to promote more effective self-healing [108]. After comparing silicon particles with different size distributions, the authors concluded that selection of Si particle sizes and their distributions was important for full utilization of SHP binders, and Si particles with 500 nm-1.5 µm size distribution were found to exhibit best electrochemical performance (high CE, stable cycling performance and low cost). As for the Si (500 nm)-SHP/carbon black (Si-SHP/CB) electrode, its initial delithiation capacity was ~2600 mAh/g and the capacity retention was \sim 80% after 550 cycles, while the first cycle CE was about 88%. Besides, such Si-SHP/CB electrode with a high mass loading of 1.13 mg_{si}/cm² exhibited an initial areal capacity of about 3.22 mAh/cm² at 0.1 mA/cm², and maintained a high areal capacity of 2.72 mAh/cm² at 0.3 mA/cm^2 after $\sim 120 \text{ cycles}$. While the same Si-based electrodes with CMC or PVDF as binder displayed rapid capacity loss after a few cycles.

4. Conclusions and perspectives

Silicon is a promising anode material for boosting the energy density of LIBs owing to its high theoretical capacity and low discharge potential. However, significant drawback of huge volume expansion upon lithiation results in poor cyclic stability of Si anodes. Such challenge has been an urgent issue, which needs to be overcomed before practical application. Si-C hybrid materials combining high electron conductivity and stability of carbon and high specific capacity of silicon, have attracted a great deal of attentions as ideal anode replacements of graphite in next-generation LIBs. Over last few years, the technical issues of Si/C anodes have been identified through multidisciplinary research efforts, and the major issues have been addressed by rational designs to demonstrate stable cycling performance as well as high capacity retention. The most significant results obtained for these Si/C materials have been classified and summarized in Table 1. Nevertheless, there are still questions remaining to be answered before the practical application of Si/C based electrodes in high energy density and high power density devices. So far, most of the researches are focused on gravimetric capacities and cycle stability of Si/C electrodes. Given the large inner void, high porosity, and huge specific surface area, most of hierarchically Si/C structures (such as yolk-shell, porous, graphene-supported sandwich structure, and 1D morphology) usually have very low tap densities, consequently resulting in low volumetric capacities and limiting energy density of the whole cell. Besides, the introduction of carbon matrix allows a limited improvement in irreversible capacity loss in the first cycle and the initial coulombic efficiency, which is far away from the commercial graphite. Furthermore, the synthesis methods for these well-engineered Si/C structures are often very elaborate and, in some cases, the addition of expensive CNTs, CNFs and graphene is sought, accounting for their high cost and difficulty to scale up for mass production. Up to now, the Si/graphite/pyrolytic carbon composites seem easy for industrialization, which have drawn tremendous attentions of many corporations. Due to the strict limitation of volume variation for practical devices, it is practical

for the Si/graphite/pyrolytic carbon composites based anodes to achieve 450–600 mAh/g (3–6 mAh/cm²) with high coulombic efficiency and good cyclic performance.

In the future, continued advancements in the following six directions will be essential for viable LIBs applications of these Si/Cbased materials and thus we anticipate that these areas will attract extensive research efforts in the next several years. (1) Current understanding of the lithium reaction mechanisms in Si/C composites, especially the lithiation/delithiation reactions in diverse microstructures, are not fully validated. It is critically important to quantitatively explore the lithiation and delithiation processes to provide invaluable data for designing and optimizing Si/C anode composites. Further work is required to understand the lithium ion transport kinetics within the Si/C electrode, especially the interfacial reactions between silicon and carbon as well as the electrode and electrolyte; (2) In consideration of real applications of LIBs, the gravimetric and volumetric capacities (related to material tap density) of Si/C electrodes should be taken into account simultaneously during the designing and fabricating processes, besides a few well-designed Si anodes (pomegranate-inspired Si design, microsized porous Si and graphene-supported etc.); (3) Further research is needed to improve rate performance of Si/C based electrodes in order to make these batteries feasible for high power applications; (4) The fabrication cost will inevitably become a formidable issue influencing the practical application of Si/C-based anodes. Substantial process improvements are needed to scale up the production of Si/C composite materials with excellent performance and develop simpler, reliable, and cost-effective solutions that would simplify the elaborate electrode fabrication techniques; (5) Prelithiation is an exceedingly effective method to enhance the initial coulombic efficiency of Si/C anodes. Researching low-cost and stable processability of lithium metal powders and exploiting new prelithiation technologies with simple process and facile industrialization are desiderate; (6) Novel electrolyte additives and polymer binders should also be developed. The addition of appropriate electrolyte additives can facilitate the formation of a thin and stable SEI layer, contributing to the cycling stability and charge efficiency of LIBs full cells, while the binders have an impact on the adhesion between current collectors and active materials as well as the integrity of electrode upon cycling. In future, further improvements will probably be achieved by simultaneously introducing new concepts of materials synthesis and hierarchical structure construction. We believe that improvements in the battery performance and the real applications of Si/C-based LIBs are on the near horizon.

References

- [1] J.M. Tarascon, M. Armand, Nature 414 (2001) 359-367.
- [2] M.M. Thackeray, C. Wolverton, E.D. Isaacs, Energy Environ. Sci. 5 (2012) 7854–7863.
- [3] M.N. Obrovac, L.J. Krause, J. Electrochem. Soc. 154 (2007) A103-A108.
- [4] M. Ashuri, Q. He, L.L. Shaw, Nanoscale 8 (2016) 74-103.
- [5] J.P. Maranchi, A.F. Hepp, A.G. Evans, N.T. Nuhfer, P.N. Kumta, J. Electrochem. Soc. 153 (2006) A1246–A1253.
- [6] X. Su, Q. Wu, J. Li, X. Xiao, A. Lott, W. Lu, B.W. Sheldon, J. Wu, Adv. Energy Mater. 4 (2013) 375–379.
- [7] L. Liu, J. Lyu, T. Li, T. Zhao, Nanoscale 8 (2016) 701-722.
- [8] F.H. Du, K.X. Wang, J.-S. Chen, J. Mater. Chem. A 4 (2016) 32-50.
- [9] X.H. Liu, L. Zhong, S. Huang, S.X. Mao, T. Zhu, J.Y. Huang, ACS Nano 6 (2012) 1522–1531.
- [10] D. Wang, M. Gao, H. Pan, J. Wang, Y. Liu, J. Power Sources 256 (2014) 190–199.
- [11] M.L. Terranova, S. Orlanducci, E. Tamburri, V. Guglielmotti, M. Rossi, J. Power Sources 246 (2014) 167–177.
- [12] J. Saint, M. Morcrette, D. Larcher, L. Laffont, S. Beattie, J.P. Peres, D. Talaga, M. Couzi, J.M. Tarascon, Adv. Funct. Mater. 17 (2010) 1765–1774.
- [13] F. Luo, B. Liu, J. Zheng, G. Chu, K. Zhong, H. Li, X. Huang, L. Chen, J. Electrochem. Soc. 162 (2015) A2509–A2528.
- [14] T. Zhang, L. Fu, J. Gao, L. Yang, Y. Wu, H. Wu, Pure Appl. Chem. 78 (2006) 1889–1896.
- 15] Y. Hwa, W.S. Kim, S.H. Hong, H.J. Sohn, Electrochim. Acta 71 (2012) 201–205.
- [16] Y. Liu, Z.Y. Wen, X.Y. Wang, A. Hirano, N. Imanishi, Y. Takeda, J. Power Sources 189 (2009) 733–737.

- [17] R. Zhou, H. Guo, Y. Yang, Z. Wang, X. Li, Y. Zhou, J. Alloys Compd. 689 (2016) 130-137.
- [18] D. Shao, D. Tang, Y. Mai, L. Zhang, J. Mater. Chem. A 1 (2013) 15068–15075.[19] H.M. Jeong, S.Y. Lee, W.H. Shin, J.H. Kwon, A. Shakoor, T.H. Hwang, S.Y. Kim, B.S. Kong, J.-S. Seo, Y.M. Lee, J.K. Kang, J.W. Choi, RSC Adv. 2 (2012) 4311–4318.
- [20] H.C. Tao, X.L. Yang, L.L. Zhang, S.B. Ni, Ionics 20 (2014) 1547-1552.
- [21] X.Y. Zhou, J.J. Tang, J. Yang, J. Xie, L.L. Ma, Electrochim. Acta 87 (2013) 663-668.
- [22] H. Tao, L.Z. Fan, W.L. Song, M. Wu, X. He, X. Qu, Nanoscale 6 (2014) 3138-3142
- [23] J. Yang, Y.X. Wang, S.L. Chou, R. Zhang, Y. Xu, J. Fan, W.X. Zhang, H. Kun Liu, D. Zhao, S. Xue Dou, Nano Energy 18 (2015) 133–142.
- [24] J. Xie, L. Tong, L. Su, Y. Xu, L. Wang, Y. Wang, J. Power Sources 342 (2017) 529-536.
- [25] Z. Sun, S. Tao, X. Song, P. Zhang, L. Gao, J. Electrochem. Soc. 162 (2015) A1530-A1536.
- [26] L.Y. Yang, H.Z. Li, J. Liu, Z.Q. Sun, S.S. Tang, M. Lei, Sci. Rep. 5 (2015) 1-9.
- [27] L. Su, J. Xie, Y. Xu, L. Wang, Y. Wang, M. Ren, PCCP 17 (2015) 17562–17565.
- [28] Y. Ma, H. Tang, Y. Zhang, Z. Li, X. Zhang, Z. Tang, J. Alloys Compd. 704 (2017) 599-606
- [29] N. Liu, Z. Lu, J. Zhao, M.T. McDowell, H.W. Lee, W. Zhao, Y. Cui, Nat. Nanotechnol. 9 (2014) 187-192.
- [30] D. Lin, Z. Lu, P.C. Hsu, H.R. Lee, N. Liu, J. Zhao, H. Wang, C. Liu, Y. Cui, Energy Environ. Sci. 8 (2015) 2371-2376.
- [31] M.S. Wang, L.Z. Fan, M. Huang, J. Li, X. Qu, J. Power Sources 219 (2012) 29-35.
- [32] Q. Li, L. Yin, X. Gao, RSC Adv. 5 (2015) 35598-35607.
- [33] H.C. Tao, L.Z. Fan, X. Qu, Electrochim. Acta 71 (2012) 194-200.
- [34] Y. Chen, N. Du, H. Zhang, D. Yang, CrystEngComm 19 (2017) 1220–1229.
- [35] I. Hong, B. Scrosati, F. Croce, Solid State Ionics 232 (2013) 24-28.
- [36] Z.L. Xu, Y. Gang, M.A. Garakani, S. Abouali, J.Q. Huang, J.K. Kim, J. Mater. Chem. A 4 (2016) 6098-6106.
- [37] Z. Zhang, Y. Wang, W. Ren, Q. Tan, Y. Chen, H. Li, Z. Zhong, F. Su, Angew. Chem. Int. Ed. 53 (2014) 5165-5169.
- [38] H. Tian, X. Tan, F. Xin, C. Wang, W. Han, Nano Energy 11 (2015) 490-499.
- [39] Y. Liu, X. Guo, J. Li, Q. Lv, T. Ma, W. Zhu, X. Qiu, J. Mater. Chem. A 1 (2013) 14075-14079.
- [40] X. Ma, M. Liu, L. Gan, P.K. Tripathi, Y. Zhao, D. Zhu, Z. Xu, L. Chen, PCCP 16 (2014) 4135-4142
- [41] Y. Song, L. Zuo, S. Chen, J. Wu, H. Hou, L. Wang, Electrochim. Acta 173 (2015) 588-594.
- [42] M. Sohn, D.S. Kim, H.I. Park, J.H. Kim, H. Kim, Electrochim. Acta 196 (2016)
- 197-205 [43] M. Gauthier, D. Mazouzi, D. Reyter, B. Lestriez, P. Moreau, D. Guyomard,
- L. Roué, Energy Environ. Sci. 6 (2013) 2145-2155. [44] Z. Lu, N. Liu, H.W. Lee, J. Zhao, W. Li, Y. Li, Y. Cui, ACS Nano 9 (2015)
- 2540-2547. [45] B. Jiang, S. Zeng, H. Wang, D. Liu, J. Qian, Y. Cao, H. Yang, X. Ai, ACS Appl.
- Mater. Interfaces 8 (2016) 31611-31616. [46] S.J. Lee, H.J. Kim, T.H. Hwang, S. Choi, S.H. Park, E. Deniz, D.S. Jung, J.W. Choi,
- Nano Lett. 17 (2017) 1870-1876. [47] Y. Zhang, Y. Jiang, Y. Li, B. Li, Z. Li, C. Niu, J. Power Sources 281 (2015)
- 425-431.
- [48] B. Kim, Solid State Ionics 172 (2004) 33-37.
- [49] M. Holzapfel, H. Buqa, W. Scheifele, P. Novák, F.M. Petrat, Chem. Commun. 12
- [50] M.K. Datta, P.N. Kumta, J. Power Sources 158 (2006) 557-563.
- [51] J.H. Lee, W.J. Kim, J.Y. Kim, S.H. Lim, S.M. Lee, J. Power Sources 176 (2008) 353-358.
- [52] H. Wang, J. Xie, S. Zhang, G. Cao, X. Zhao, RSC Adv. 6 (2016) 69882-69888.
- [53] J. Shu, H. Li, R. Yang, Y. Shi, X. Huang, Electrochem. Commun. 8 (2006) 51-54.
- [54] T. Kim, Y.H. Mo, K.S. Nahm, S.M. Oh, J. Power Sources 162 (2006) 1275-1281.
- [55] M. Zhang, X. Hou, J. Wang, M. Li, S. Hu, Z. Shao, X. Liu, J. Alloys Compd. 588 (2014) 206-211.
- [56] W. Wang, P.N. Kumta, ACS Nano 4 (2010) 2233-2241.
- [57] A. Gohier, B. Laïk, K.H. Kim, J.L. Maurice, J.P. Pereira-Ramos, C.S. Cojocaru, P.T. Van, Adv. Mater. 24 (2012) 2592-2597.
- [58] L. Mangolini, J. Vac. Sci. Technol. B, Nanotechnol. Microelectron. Mater. Process. Meas. Phenom. 31 (2013) 020801.
- [59] T.H. Hwang, Y.M. Lee, B.S. Kong, J.S. Seo, J.W. Choi, Nano Lett. 12 (2012) 802-807
- [60] Y. Chen, Y. Hu, Z. Shen, R. Chen, X. He, X. Zhang, Y. Li, K. Wu, J. Power Sources 342 (2017) 467-475.
- [61] B. Wang, X. Li, X. Zhang, B. Luo, Y. Zhang, L. Zhi, Adv. Mater. 25 (2013) 3560-3565.
- [62] J.K. Yoo, J. Kim, Y.S. Jung, K. Kang, Adv. Mater. 24 (2012) 5452-5456.
- [63] Z. Lu, T. Wong, T.W. Ng, C. Wang, RSC Adv. 4 (2014) 2440-2446.
- [64] J. Liu, N. Li, M.D. Goodman, H.G. Zhang, E.S. Epstein, B. Huang, Z. Pan, J. Kim, J.H. Choi, X. Huang, J. Liu, K.J. Hsia, S.J. Dillon, P.V. Braun, ACS Nano 9 (2015) 1985-1994.
- [65] M. Zamfir, H. Nguyen, E. Moyen, Y. Lee, D. Pribat, J. Mater. Chem. A 1 (2013) 9566-9586.

- [66] D. Ma, Z. Cao, A. Hu, Nano Micro. Lett. 6 (2014) 347-358.
- [67] S.L. Chou, J.Z. Wang, M. Choucair, H.K. Liu, J.A. Stride, S.X. Dou, Electrochem. Commun. 12 (2010) 303–306.
- [68] J.K. Lee, K.B. Smith, C.M. Hayner, H.H. Kung, Chem. Commun. 46 (2010) 2025-2027.
- [69] M. Ko, S. Chae, S. Jeong, P. Oh, J. Cho, ACS Nano 8 (2014) 8591-8599.
- [70] X. Zuo, J. Zhu, P. Müller-Buschbaum, Y.J. Cheng, Nano Energy 31 (2016) 113-143.
- [71] I.H. Son, J.H. Park, S. Kwon, S. Park, M.H. Rümmeli, A. Bachmatiuk, H.J. Song,
- J. Ku, J.W. Choi, J. Choi, Nat. Commun. 6 (2015) 7393–7401. [72] J. Luo, X. Zhao, J. Wu, H.D. Jang, H.H. Kung, J. Huang, J. Phys. Chem. Lett. 3 (2012) 1824–1829.
- [73] X. Zhou, Y.X. Yin, L.J. Wan, Y.G. Guo, Adv. Energy Mater. 2 (2012) 1086–1090.
- [74] W. Yue, S. Jiang, W. Huang, Z. Gao, J. Li, Y. Ren, X. Zhao, X. Yang, J. Mater. Chem. A 1 (2013) 6928–6933.
- [75] T. Mori, C.J. Chen, T.F. Hung, S.G. Mohamed, Y.Q. Lin, H.Z. Lin, J.C. Sung, S.F. Hu, R.S. Liu, Electrochim. Acta 165 (2015) 166-172.
- [76] X. Liu, J. Zhang, W. Si, L. Xi, B. Eichler, C. Yan, O.G. Schmidt, ACS Nano 9 (2015) 1198-1205.
- [77] M. Zhou, X. Li, B. Wang, Y. Zhang, J. Ning, Z. Xiao, X. Zhang, Y. Chang, L. Zhi, Nano Lett. 15 (2015) 6222-6228.
- [78] M. Zhou, T. Cai, F. Pu, H. Chen, Z. Wang, H. Zhang, S. Guan, ACS Appl. Mater. Interfaces 5 (2013) 3449-3455.
- [79] R. Yi, J. Zai, F. Dai, M.L. Gordin, D. Wang, Nano Energy 6 (2014) 211-218.
- [80] J. Wu, X. Qin, H. Zhang, Y.B. He, B. Li, L. Ke, W. Lv, H. Du, Q.H. Yang, F. Kang, Carbon 84 (2015) 434-443.
- [81] D.A. Agyeman, K. Song, G.H. Lee, M. Park, Y.M. Kang, Adv. Energy Mater. 6 (2016) 1600904.
- [82] H. Zhou, X. Wang, D. Chen, ChemSusChem 8 (2015) 2737-2744.
- [83] M.W. Forney, M.J. Ganter, J.W. Staub, R.D. Ridgley, B.J. Landi, Nano Lett. 13 (2013) 4158-4163.
- [84] K. Yao, R. Liang, J.P. Zheng, J. Electrochem. Energy Convers. Storage 13 (2016) 61 - 73.
- [85] Q. Pan, P. Zuo, T. Mu, C. Du, X. Cheng, Y. Ma, Y. Gao, G. Yin, J. Power Sources 347 (2017) 170-177
- [86] H.J. Kim, S. Choi, S.J. Lee, M.W. Seo, J.G. Lee, E. Deniz, Y.J. Lee, E.K. Kim, J.W. Choi, Nano Lett. 16 (2016) 282-288.
- [87] Z. Cao, P. Xu, H. Zhai, S. Du, J. Mandal, M. Dontigny, K. Zaghib, Y. Yang, Nano Lett. 16 (2016) 7235-7240.
- [88] L. Chen, K. Wang, X. Xie, J. Xie, J. Power Sources 174 (2007) 538-543.
- [89] L. Chen, K. Wang, X. Xie, J. Xie, Electrochem. Solid-State Lett. 9 (2006) A175-A178.
- [90] G.B. Han, J.N. Lee, J.W. Choi, J.K. Park, Electrochim. Acta 56 (2011) 8997–9003.
- [91] Y. Li, G. Xu, Y. Yao, L. Xue, S. Zhang, Y. Lu, O. Toprakci, X. Zhang, J. Solid State Electrochem. 17 (2013) 1393-1399.
- [92] G.B. Han, M.H. Ryou, K.Y. Cho, M.L. Yong, J.K. Park, J. Power Sources 195 (2010) 3709-3714
- [93] N.S. Choi, K.H. Yew, K.Y. Lee, M. Sung, H. Kim, S.S. Kim, J. Power Sources 161 (2006) 1254-1259.
- [94] C. Xu, F. Lindgren, B. Philippe, M. Gorgoi, F. Björefors, K. Edstrom, T. Gustafsson, Chem. Mater. 27 (2015) 549-554
- [95] X. Chen, X. Li, D. Mei, J. Feng, M.Y. Hu, J. Hu, M. Engelhard, J. Zheng, W. Xu, J. Xiao, ChemSusChem 7 (2013) 549-554.
- [96] V. Etacheri, O. Haik, Y. Goffer, G.A. Roberts, I.C. Stefan, R. Fasching, D. Aurbach, Langmuir ACS J. Surf. Colloids 28 (2012) 965-976.
- [97] D. Shao, H. Zhong, L. Zhang, Chem. Electro. Chem. 1 (2014) 1679-1687.
- [98] A. Magasinski, B. Zdyrko, I. Kovalenko, B. Hertzberg, R. Burtovyy, C.F. Huebner, T.F. Fuller, I. Luzinov, G. Yushin, ACS Appl. Mater. Interfaces 2 (2010) 3004-3010.
- [99] L. Zhang, L. Zhang, L. Chai, P. Xue, W. Hao, H. Zheng, J. Mater. Chem. A 2 (2014) 19036–19045.
- [100] J. Yoon, D.X. Oh, C. Jo, J. Lee, D.S. Hwang, PCCP 16 (2014) 25628-25635.
- [101] I. Kovalenko, B. Zdyrko, A. Magasinski, B. Hertzberg, Z. Milicev, R. Burtovyy, I. Luzinov, G. Yushin, Science 334 (2011) 75-79.
- [102] M. Wu, X. Xiao, N. Vukmirovic, S. Xun, P.K. Das, X. Song, P. Olalde-Velasco, D. Wang, A.Z. Weber, L.W. Wang, V.S. Battaglia, W. Yang, G. Liu, J. Am. Chem. Soc. 135 (2013) 12048-12056.
- [103] M.H. Ryou, J. Kim, I. Lee, S. Kim, Y.K. Jeong, S. Hong, J.H. Ryu, T.S. Kim, J.K. Park, H. Lee, J.W. Choi, Adv. Mater. 25 (2013) 1571-1576.
- [104] B. Koo, H. Kim, Y. Cho, K.T. Lee, N.-S. Choi, J. Cho, Angew. Chem. Int. Ed. 51 (2012) 8762-8767.
- [105] J. Song, M. Zhou, R. Yi, T. Xu, M.L. Gordin, D. Tang, Z. Yu, M. Regula, D. Wang, Adv. Funct. Mater. 24 (2014) 5904-5910.
- [106] J. Liu, Q. Zhang, Z.Y. Wu, J.H. Wu, J.T. Li, L. Huang, S.G. Sun, Chem. Commun. 50 (2014) 6386-6389.
- [107] T. Yim, S.J. Choi, J.H. Park, W. Cho, Y.N. Jo, T.H. Kim, Y.J. Kim, PCCP 17 (2015) 2388-2393.
- [108] Z. Chen, C. Wang, J. Lopez, Z. Lu, Y. Cui, Z. Bao, Adv. Energy Mater. 5 (2015) 1401826.
- [109] C. Wang, H. Wu, Z. Chen, M.T. McDowell, Y. Cui, Z. Bao, Nat Chem 5 (2013) 1042-1048.